Archimer
http://archimer.ifremer.fr

Sex-Specific Regulation of AMP-Activated Protein Kinase (AMPK) in the Pacific Oyster *Crassostrea gigas*[1]

Eric Guévélou[a], Arnaud Huvet[a], Clara E. Galindo-Sánchez[b], Massimo Milan[c], Virgile Quillien[a], Jean-Yves Daniel[a], Claudie Quéré[a], Pierre Boudry[a], and Charlotte Corporeau[a, *]

[a] Ifremer, Laboratoire des Sciences de l'Environnement Marin (UMR 6539, LEMAR), Plouzané, France
[b] Centro de Investigación Científica y de Educación Superior de Ensenada (CICESE), Departamento de Biotecnología Marina, Ensenada, Baja California, México
[c] University of Padova, Department of Comparative Biomedicine and Food Science, Legnaro (Padova), Italy

*: Corresponding author : Charlotte Corporeau, email address : Charlotte.Corporeau@ifremer.fr

Abstract:

The hermaphrodite Pacific oyster *Crassostrea gigas* displays a high energy allocation to reproduction. We studied the expression of AMP-activated protein kinase (AMPK) during gametogenesis in the gonad and characterized the mRNA sequences of the *AMPK* subunits: the *AMPK* alpha mRNA sequence was previously characterized; we identified *AMPK* beta, *AMPK* gamma, and mRNAs of putative AMPK-related targets following bioinformatics mining on existing genomic resources. We analyzed the mRNA expression of the *AMPK* alpha, beta, and gamma subunits in the gonads of male and female oysters through a reproductive cycle, and we quantified the mRNA expression of genes belonging to fatty acid and glucose metabolism. *AMPK* alpha mRNA levels were more abundant in males at the first stage of gametogenesis, when mitotic activity and the differentiation of germinal cells occur, and were always more abundant in males than in females. Some targets of fatty acid and glucose metabolism appeared to be correlated with the expression of *AMPK* subunits at the mRNA level. We then analyzed the sex-specific AMPK activity by measuring the phosphorylation of the catalytic AMPK alpha protein and its expression at the protein level. Both the amount of AMPK alpha protein and threonine 172 phosphorylation appeared to be almost totally inhibited in mature female gonads at stage 3, at the time when accumulation of reserves in oocytes was promoted, while it remained at a high level in mature spermatozoa. Its activation might play a sex-dependent role in the management of energy during gametogenesis in oyster.

Keywords: AMP-activated protein kinase ; *Crassostrea gigas* ; Gametogenesis ; marine bivalve ; reproduction

1. Introduction

In the Lophotrochozoa clade of bilaterian animals, some marine bivalves such as the Pacific oyster *Crassostrea gigas* have a unique reproductive cycle. *C. gigas* is an irregular successive hermaphrodite, meaning that most individuals first develop as males [1] and may then change sex between different reproductive seasons [2]. In temperate regions, *C. gigas* exhibits a seasonal reproductive cycle, mainly driven by temperature and food availability [3]. The *C. gigas* gonad is a diffuse and non-permanent tissue composed of somatic cells and germ cells that surround the digestive gland [4]. Consequently, oyster gonad is a mixed tissue including storage tissue, smooth muscle fibers and infiltrated hemocytes. The primary gonad of *C. gigas* contains germ cells that derive from germinal stem cells produced by early differentiation of primordial germ cells during embryogenesis [4]. During the initial stage of gametogenesis (*i.e.* Stage 0), small clusters of self-renewing stem cells are scattered in conjunctive tissue [4, 5]. At this stage, the sex of individuals cannot be determined, even by histological observations. During stage 1, germ cells divide by mitosis and differentiate to produce a large number of gonia (gonial proliferation) [3, 5-9]. From this stage, the sex of individuals can be determined using histological methods. The mitotic activity of the cells induces the expansion of tubules that invaginate the storage tissue surrounding the digestive system. Gonads classified as stage 2 have maturating germ cells in developing gonadic tubules that grow and ramify at the expense of the storage tissue [7, 10, 11]. At stage 3, gonads are fully mature and completely filled due to the confluence of gonadic tubules [3, 6, 7].

In *C. gigas*, two peptides related to "gonadotropin-releasing hormone" (GnRH) and five Neuropeptide Y receptors might be involved in the management of energy needs for reproduction [12, 13]. An increase in 17β-estradiol was observed during gametogenesis, suggesting its role in vitellogenesis [14], and an estrogen receptor is predominantly expressed in mature animals [15]. Moreover, several elements of the insulin signaling pathway were identified in *C. gigas*: an "insulin-like peptide" ligand (ILP) expressed in the visceral ganglia and regulated during gametogenesis [16], a *C. gigas* insulin receptor-related receptor (CIR) [17], Ras oncogene, phosphatase-tensin homolog deleted on chromosome (PTEN) and p70-S6 Kinase [18]. However, no functional data are yet available for these endocrine and signaling molecules in reproduction and further analyses are needed to study their function.

Like many marine invertebrates, Pacific oysters have very high fecundity [19, 20]. Adults allocate nearly 55% of their annual energy budget to reproduction [21] and, when mature, the gonad represents up to 60% of the volume of the visceral mass [3]. Gametogenesis is a period of negative energy balance where most of the stored energy is used for gamete production [11, 22]. As a result, gametogenesis might have a major impact on several physiological functions, such as defense and growth and, therefore, on survival. In fact, reproduction has often been suggested as the potential reason why higher summer mortality occurs in oysters during reproduction [23-27], individuals with high energy investment in gametogenesis would have less energy available for maintenance and defense.

In vertebrates, the physiological mechanisms that control energy metabolism are linked with those that control reproduction through energetic signaling pathways, which integrate energy intake, storage and expenditure to allow animals to reach reproductive maturity. When these signaling pathways are deregulated, animals are less fertile [28, 29]. In the past, gonad differentiation and development in oysters were studied by measuring the expression of genes potentially involved in reproduction (for example *CG-FOXL2* [30, 31], *CG-DML* [32], vasa (termed oyvlg) [5], *OG-TGF beta* [33, 34] or elements belonging to the insulin pathway [16-18] and recently by a genome-wide expression profiling that identified gonad- and sex-specific genes and potential markers of early sex differentiation in *C. gigas* [35]. Despite this work, however, our understanding of the mechanisms of the regulation of gonad development versus storage tissue is still limited [36].

In vertebrates, the energetic signaling pathway of AMP-dependent kinase (AMPK) plays a major role in the balance between reproduction and energy metabolism to control gametogenesis [37, 38].

AMPK is an heterotrimeric kinase composed of a catalytic alpha-subunit and two regulatory subunits, beta and gamma. The genes encoding the three subunits of AMPK are highly conserved in eukaryotic species for which complete genome sequences are available, including vertebrates, invertebrates, plants, fungi, and protozoa [39]. In humans, two or three genes encode each subunit, giving rise to 12 possible heterotrimeric combinations, with spliced variants further increasing the potential diversity of AMPK proteins [40]. AMPK activation requires the presence of all three subunits [41] and its kinase activity is regulated at the post-translational level. Many phosphorylation sites have been described in AMPK alpha and beta subunits [42-44]. AMPK alpha threonine 172 has been identified as the determinant and required phosphorylation site for activation of AMPK kinase [42, 45, 46]. A high cellular ratio of AMP/ATP triggers the phosphorylation and activation of AMPK [47]. Once activated by low energy status, AMPK rapidly phosphorylates and modulates a wide array of downstream targets, mainly glucose and fatty acid metabolic enzymes. AMPK stimulates ATP-producing catabolic pathways, such as lipolysis, glycolysis and glucose uptake, while it inhibits ATP-consuming anabolic pathways, such as glycogen synthesis and lipogenesis [48].

Most of AMPK studies have been conducted in somatic cells of vertebrates and this study first explores AMPK during gametogenesis in an invertebrate species, the Pacific oyster *Crassostrea gigas*. We quantified the protein expression and activity status of AMPK in the gonadic tissue of male and female oysters, reared under natural conditions. We also studied correlations during the time-course of gametogenesis between AMPK activation and mRNA expression of several genes presumed to be involved in energy regulation.

2. Material and methods

2.1. Animals

Oysters were produced in March 2005 at the Ifremer hatchery in La Tremblade (Charente-Maritime, France), from wild oyster genitors (progeny "G4t2n" as described in [49]). Juveniles were then reared at the Ifremer Bouin nursery (Pays de la Loire, France). In April 2006, the one-year-old oysters were put in standard field culture (300 oysters per bag, 17 bags in total) in Locmariaquer (Morbihan, France), where they were maintained for three years.

Fourteen bags were dedicated to sampling and the three remaining bags used to estimate the mortality by monthly counting of dead and live oysters. From November 2008 through June 2009, dead oysters were removed from the bags, and around 60 were collected at random from the 14 bags (5 per bag) monthly. At each sampling time, oysters were opened, the shell removed, and a 3-mm cross section of the visceral mass excised just in front of the pericardial region for histological processing and examination. The left part of the gonad was immediately frozen, crushed to a fine powder at -196°C with a Dangoumeau mill, and stored in liquid nitrogen for later analyses.

2.2. Histology

For all studied individuals, the 3-mm cross sections were immediately fixed in modified Davidson's solution [50] at 4°C for 48 h. Sections were dehydrated in ascending ethanol solutions, cleared with with Microclearing (Diapath) (a xylene substitute) and embedded in paraffin wax. Sections of 5 µm thickness were cut, mounted on glass slides and stained with Harry's hematoxylin-eosin Y [51]. The histological slides were examined under a light microscope to determine the sex and the gametogenic stage of each individual, according to the reproductive scale reported by Steele and Mulcahy (1999) [52].

The initial stage of gametogenesis, stage 0, is considered a sexual resting stage where small clusters of self-renewing stem cells appear scattered in the conjunctive tissue. At this stage, the sex

of an individual cannot be determined by histological observations. After stage 0, germ cells divide by mitosis during stage 1; meiosis occurs during stage 2; and stage 3 is the stage of ripeness when spawning can occur [5, 9, 52]. Starting from stage 1, males and females follow sex-specific differentiation for gametogenesis. Three different stages were observed for each sex and considered in the present study, as follows.

For females: Stage 1 (developing early active): Oogonia arising from stem cells along the follicle; no free oocytes. Connective tissue is very abundant. Stage 2 (developing late active): Free and attached oocytes present with distinct nuclei that stain paler than the cytoplasm. Stage 3 (ripe): Free oocytes with distinct nuclei and nucleoli.

For males: Stage 1 (developing early active): Many small follicles; spermatogonia and spermatocytes numerous, no spermatozoa. Stage 2 (developing late active): Follicle cells contain predominantly spermatids and spermatozoa; spermatozoa have a characteristic swirling pattern with tails toward follicle lumen, in centre of follicle. Stage 3 (ripe): Inter-follicular tissue and germinal epithelium are inconspicuous. Follicles filled with spermatozoa, oriented with tails toward the follicle lumen forming a characteristic swirling pattern that completely fills the follicle.

2.3. Database mining

All the genes analyzed in this study were identified from the GigasDatabase (www.sigenae.org, [53]. Homology searches obtained from GigasDatabase were confirmed, or in some cases modified, by one-by-one annotation of the selected ESTs using a blastx search [54] and protein domain conservation using ExPASy prosite [55] and SMART [56], following cDNA sequence conversion into predicted amino acids using the ExPASy translate tool [57]. Multiple alignments of predicted amino acids of oyster sequences were performed with a range of _AMPK_ sequences from vertebrates and invertebrates, including _C. gigas_ sequences released from the oyster genome project [58], using CLUSTALW [59].

2.4. Phylogenetic tree construction

BLAST searches were performed on the NCBI protein collection nr/prot database and ENSEMBL protein database (http://www.ensembl.org/index.html), using the blastx option with default settings in order to retrieve _AMPK_ beta and _AMPK_ gamma orthologs in both vertebrate and invertebrate species. For phylogenetic tree construction, all amino acid sequences (listed in Supplementary file I) were aligned using the MUSCLE program, by applying the default settings. The resulting alignment was analyzed with the Neighbor-Joining method (MEGA software, version 5.0).

2.5. Real-time PCR analyses

Total RNA of each individual was isolated using Extract-all (Eurobio), at a concentration of 1 ml / 50 mg powder. Samples were then treated with DNAse I (1 U µg $^{-1}$ total RNA, Sigma) to prevent DNA contamination. RNA quality was assessed using RNA nano chips and Agilent RNA 6000 nano reagents (Agilent Technologies, Waldbronn, Germany), according to the manufacturer's instructions. RNA concentrations were measured using an ND-1000 spectrophotometer (Nanodrop Technologies) at 260 nm, using the conversion factor 1OD = 40µg mL^{-1} RNA. From 2 µg total RNA, RT-PCR amplifications were carried out for 10 mRNA as described in [4]. In the present study, amplification of the housekeeping gene _elongation factor I_ (_efI_) cDNA (primers in [4] was used as an internal control for gene expression. Indeed, this gene presented a steady-state level of expression (CV = 3.1%) and we did not observe any significant difference between Cq values for _efI_ between the treatments (two-way ANOVA: F = 1.97; _p_ = 0.084). PCR efficiency (E) was estimated for each primer pair by constructing standard curves to ensure that E ranged from 98 to 102 %. Real-time PCR amplifications were then carried out in triplicate, with 5 µl cDNA (1/10 dilution) in a total volume of 15 µl, using the iQ SYBR Green Supermix (Biorad) and an Icycler (Biorad) (protocol in [60]. Samples were deposited in random positions in each plate. Each run included a cDNA reference,

negative controls (each total RNA sample with DNAse I treatment), and blank controls (water) analyzed for each primer pair. Melting curve analysis was systematically performed for all genes in order to verify the specificity of the PCR product. For a studied gene "i", results were expressed as $2^{-\Delta\Delta Cq}$ [61] with $\Delta Cq = Cq\ (i) - Cq\ (efl)$ and $\Delta\Delta Cq = \Delta Cq$ of cDNA sample - $\Box Cq$ of the cDNA reference. A specific set of primer pairs designed to amplify parts of the different genes (*AMPK alpha, AMPK beta, AMPK gamma, ACC, NCOA4, CAMK4, SREBP1, PI3K, AKT* and *CREB*). The primer sequences were designed using Primer 3 software[62], their accession number and corresponding PCR efficiencies are listed in Table 1.

2.6. Total protein extraction

For each individual, 150 mg of powdered tissue were homogenized in a lysis buffer (150 mM NaCl, 10 mM Tris, pH 7.4, 1 mM EDTA, 1 mM EGTA, 1% Triton X-100, 0.5% Igepal; pH 8.8 at 4°C) enriched with phosphatase and protease inhibitors (5 ml phosphatase inhibitor cocktail II, 1 tablet of "cOmplete EDTA-free protease inhibitor cocktail" per 25 ml). Total proteins were then extracted as described in [63]. Briefly, total protein lysates were obtained after homogenization with an Ultra-Turax and soft centrifugation at 3,000 g for 1 h at 4°C. The lipid layer was in the upper phase and was easily eliminated by pipetting. The interphase, which contained the proteins, was collected and the small pellet of cell debris was discarded. The interphase was then centrifuged at 10,000 g for 45 min at 4°C to ensure total lipid depletion. The interphase was collected, aliquoted and stored at -80°C. For each lysate, the total protein content was quantified using a DC protein assay (Bio-Rad) with 96-well microplates (Nunc) in a microplate reader (Bio-Tek® Synergy) and KC4 v3 software to compare results with a calibration curve of standard proteins (bovine serum albumin) provided with the DC protein assay kit. Each protein lysate was then adjusted to a final concentration of 3 mg ml $^{-1}$ by adding lysis buffer, and stored at -80°C until later analysis.

2.7. Western-blot analyses

Denaturation, gel migration and transfer were performed using the same protocol as [56]. Immunodetections were performed with a rabbit monoclonal antibody anti-AMPK alpha (dilution 1:1000; CST #2603; Ozyme, Cell Signaling Technology), a mouse monoclonal antibody anti-AMPK alpha (dilution 1:1000; CST #2793; Ozyme, Cell Signaling Technology) and a rabbit monoclonal antibody anti-phospho-threonine 172 AMPK alpha (dilution 1:1000; CST #2535; Ozyme, Cell Signaling Technology); Heterologous antibodies CST #2603 and CST #2793 directed against AMPK alpha had already been validated for the recognition of the truncated AMPK alpha isoforms or the entire AMPK alpha, respectively [64]. Moreover, Cell Signaling Technology technical services blasted and confirmed that the antigenic region of the commercially available anti-phospho-threonine 172 AMPK alpha antibody was present at 100 % in the *C. gigas* protein (Cell Signaling Technology; personal communication). Blots were then revealed using a horseradish peroxidase-linked secondary goat anti-rabbit antibody (dilution 1:5000) and a horseradish peroxidase (HRP) detection kit (Biorad). The relative amount of protein detected was quantified using MULTI-ANALYST software (Biorad) with the background signal removed. The value obtained was expressed in OD/mm^2 and represents the band intensity expressed as mean count per pixel, multiplied by the band surface. To ensure that identical amounts of total protein samples were loaded into the gels, membranes were dehybridized for 1 h at room temperature in dehybridizing buffer (100 mM glycine, 100 mM NaCl pH 3.2), and rehybridized with an anti-histone H3 antibody (dilution 1:5000; # 9175; Ozyme, Cell Signaling Technology), as described in [65].

2.8. Statistical analyses

Statgraphics software (StatPoint Technologies, Inc.) was used for all statistical analyses. The normality of the data was checked by the Kolmogorov-Smirnov test. The homoscedasticity of the data was checked by Bartlett's test. Analysis of variance (ANOVA) was performed to detect whether differences in the data were significant. Student-Newman-Keul multiple comparison of sample means with a 95% confidence interval was used to compare between stages of gametogenesis for

the same sex. For comparison between sexes at the same stage of gametogenesis, we used two-sided t-tests of two independent samples with a significance threshold of $p < 0.05$ (*), $p < 0.01$ (**) or $p < 0.001$ (***). Results are expressed as mean ± standard error (SE). A matrix of Spearman correlations coefficients was made between all variables with adjusted Holm-Bonferonni correction p-values.

3. Results

3.1. Characterization of AMPK beta and gamma subunits

AMPK beta subunit: Among the *C. gigas* EST sequences available in GigasDatabase [53], we identified several contigs annotated as *AMPK* beta that were not automatically merged into a single contig due to insufficient alignment score and/or overlap length. Multiple alignments of these contigs (Sigenae accession numbers CU991642, FU6OSJA01AUVKV, FU6OSJA01BDGCM) were performed manually using ClustalW. This allowed us to correct the sequence avoiding some false stop codons created by sequencing errors and thus create a new contig (Fig. 1 A). Blasting the recently published complete genome sequence of *C. gigas* showed only one significant result that matched with our *AMPK* beta mRNA sequence (GenBank accession number EKC39833; [58]). The 807 base pair cDNA obtained encoded an entire AMPK beta protein of 268 amino acids and 30 kDa that showed more than 65% conservation with AMPK beta subunits in other species. The phylogenetic placement of this sequence in relation to *AMPK* beta sequences found in other species showed that *C. gigas AMPK* beta is not strongly linked to the other *AMPK* beta isoforms already described (Fig 1 B). The N-terminal myristoylation site, responsible for membrane binding [43, 66] is present (Fig. 1 A). Both the glycogen-binding domain (beta-GBD), which is responsible for binding AMPK to glycogen [67, 68], and the alpha gamma-subunit binding sequence (alpha gamma-SBS), which is responsible for binding AMPK beta to AMPK alpha and AMPK gamma [69], were conserved in *C. gigas*. Comparing amino acid sequences, *C. gigas* AMPK beta GBD and alpha gamma-SBS share 62% and 40%, respectively, similarity with *Homo sapiens* AMPK beta2. Several serine phosphorylation sites have been characterized in the AMPK beta subunit [43, 44, 66]. In *C. gigas*, the serine 24/25, serine 96 and serine 101 phosphorylation sites are missing, while serine 108 (positioned at serine 102 in *C. gigas* AMPK beta) and serine 182 phosphorylation sites are conserved (Fig. 1 A).

AMPK gamma subunit: Among the *C. gigas* EST sequences in GigasDatabase [53], we identified a sequence of 1,185 base pairs, corresponding to the complete *C. gigas AMPK* gamma mRNA (Sigenae accession number FU6OSJA01ADEEL). The 1,185 base pair cDNA encoded an entire AMPK gamma protein of 394 amino acids with a molecular weight of 44 kDa and showed more than 41% amino acid sequence conservation with AMPK gamma subunits from other species. This sequence has 99% identity with a *C. gigas AMPK* gamma2 mRNA subunit characterized in the complete genome sequence of *C. gigas* (GenBank accession number EKC25878; [58]). In other species, the gamma isoforms 1, 2 or 3 differ in the length of their N-terminal extensions, which are not predicted to have any domain structure [70]. The phylogenetic placement of our sequence in relation to AMPK gamma sequences found in other species suggested that *C. gigas* AMPK gamma is slightly linked to AMPK gamma2 isoforms (Fig 2 B). The four tandem repeats as cystathionine beta-synthase (CBS) motif, termed Bateman domains [71], are conserved in *C. gigas* (Fig 2 A). *Crassostrea gigas* AMPK gamma2 CBS1, CBS2, CBS3 and CBS4 have amino acid sequence similarity of more than 80%, 54%, 65%, and 52% with *H. sapiens* AMPK gamma2 CBS (GenBank accession number NP_057287), respectively.

3.2. Entire AMPK alpha, beta and gamma mRNA during gametogenesis

Based on histological examination of the gonad section, we selected 13 sexually undifferentiated oysters (stage 0) and 10 males and 10 females for each stage of gametogenesis (stages 1, 2 and 3). As shown in Figure 3, all three subunits of AMPK were expressed in gonads at all stages of

gametogenesis, in sexually undifferentiated oysters as well as in males and females. In males, entire *AMPK* alpha mRNA level was significantly higher in stage 0 and stage 1 than in the more advanced reproductive stages. In fact, males at stage 3 had entire *AMPK* alpha mRNA levels 50% lower than males at stage 1 (Fig. 3 A) while *AMPK* beta and *AMPK* gamma levels remained constant. This suggests that the behavior of *AMPK* mRNA subunits was different in male at stage 3. In fact, *AMPK* beta and *AMPK* gamma mRNA levels of males showed no significant variation during the time course of gametogenesis (Fig. 3 B and C). In females, all three *AMPK* subunits, entire *AMPK* alpha, *AMPK* beta and *AMPK* gamma, showed similar mRNA levels at stages 1, 2 and 3 (Fig. 3).

3.3. AMPK alpha protein quantity and phosphorylation during gametogenesis

3.3.1. Truncated (45 kDa) and entire (62 kDa) AMPK alpha protein amounts

Here we showed that the entire AMPK alpha and truncated AMPK alpha protein were detected in gonads of both males and females at all reproductive stages (Fig. 4). In both males and females, AMPK alpha truncated protein (45kDa) was detected at a very low level and its amount did not vary statistically during reproduction (ANOVA: $F = 1.66$; $p = 0.1540$) (Fig. 4A). The entire AMPK alpha protein (62kDa) was detected at a high level and its amount did vary statistically during reproduction (ANOVA: $F = 6.50$; $p = 0.0015$) (Fig. 4 B). In males, level of entire AMPK alpha protein (62 kDa) was constant during all stages of gametogenesis. In females, the level of entire AMPK alpha remained constant from stage 0 to stage 2 and was decreased significantly by 65 % from stage 2 to stage 3 (Fig. 4 B).

3.3.2. Threonine 172 phosphorylation of AMPK alpha (62kDa)

Using the monoclonal anti-phospho-threonine 172 AMPK alpha antibody, a single band with an apparent molecular weight of 62 kDa was obtained by SDS-PAGE (Fig. 5). This band was rapidly detected at a high level with no background in gonads of both males and females (Fig. 5). Its amount varied statistically during reproduction (ANOVA: $F = 4.52$; $p = 0.001$) (Fig. 5). In males, the level of thr172 phosphorylation of AMPK alpha was constant during all stages of gametogenesis. In females, the level of thr172 phosphorylation of AMPK alpha was constant from stage 0 to stage 2 and decreased significantly by 88 % from stage 2 to stage 3 (Fig. 5). At stage 3, thr172 phosphorylation of AMPK alpha was 11.5 fold higher in male than in female gonads. Ratio between thr172 phosphorylation of AMPK alpha and entire AMPK alpha (62 kDa) have been calculated. This ratio varied statistically during reproduction (ANOVA: $F = 2.54$; $p = 0.032$) (Fig. 5 B). In males, it was constant during all stages of gametogenesis. In females, it was constant from stage 0 to stage 2 but decreased significantly by 54 % from stage 2 to stage 3 (Fig. 5 B). At stage 3, ratio between thr172 phosphorylation of AMPK alpha and level of entire AMPK alpha (62 kDa) was 3.4 fold higher in male than in female gonads.

3.4. mRNA expression of AMPK downstream targets during gametogenesis

3.4.1. mRNAs of fatty acid metabolism

Using GigasDatabase [53], four mRNAs belonging to fatty acid metabolism were characterized in *C. gigas*. They encoded Acetyl-CoA Carboxylase (ACC), Nuclear receptor co-activator 4 (NCOA4), Calcium/Calmodulin-dependent protein Kinase type IV (CaMK4) and Sterol Regulatory Element-Binding Protein 1 (SREBP1).

The *ACC* cDNA sequence (Sigenae accession number HS120730) was identified as a 2,858-base pair sequence including the 3'UTR region (178 base pairs), but missing the 5'UTR and the beginning of the coding region. Blasting on the complete genome sequence of *C. gigas* published very recently [58] revealed that the sequence coincides (40% identity) with the *C. gigas ACC* mRNA

subunit (GenBank accession number EKC42779). The complete deduced *C. gigas* ACC protein contained 1,513 amino acids. NCOA4 sequence (GenBank accession number AM855314) was identified as a 3,520-base pair sequence. This complete cDNA sequence has a 5'UTR (266 base pairs) and 3'UTR region (1,460 base pairs) and encodes a complete *C. gigas* NCOA4 protein of 597 amino acids. This sequence is 99% similar with the *C. gigas NCOA4* mRNA subunit obtained in the complete oyster genome sequence (GenBank accession number EKC34356) and shows a conservation of N-terminal androgen receptor (AR)-associated coregulator 70. The Camk4 sequence (Sigenae accession number AM856845) was identified as a 750-base pair sequence. From blast and alignment, this cDNA sequence appears partial and is missing both 5'UTR and 3'UTR as well as start-end parts of the coding region. The partial *C. gigas* CaMK4 protein is 250 amino acids long and shows more than 59% identity with *C. gigas CAMK4* mRNA complete genome sequence (GenBank accession number EKC30614) [58]. The complete deduced *C. gigas* CAMK4 protein is 287 amino acids long. The *SREBP1* sequence (Sigenae accession number BQ426935) was identified as a 2,485-base pair sequence. The 5'UTR and the beginning of the coding region are not characterized. The 3'UTR region is 168 base pairs long. The partial *C. gigas* SREBP1 protein is 771 amino acids long and corresponds to GenBank accession number EKC21309 in the complete genome sequence (76% identity). The complete deduced *C. gigas* SREBP1 protein is 997 amino acids long.

Gene expression of these mRNAs belonging to fatty acid metabolism was assayed by real-time PCR. *ACC* mRNA relative levels were stable during gametogenesis in the two sexes (Fig. 6 A). *NCOA4* mRNA remained constant in males over the course of gametogenesis and was significantly lower than level at stage 0 (Fig. 6 B). *NCOA4* mRNA levels show a sex-specific expression. Indeed, *NCOA4* mRNA levels was significantly over-expressed in male gonad compared to female gonad in stages 1, 2 and 3. *NCOA4* mRNA (Fig.6 B) displayed a gene expression pattern similar to that of *AMPK* beta and *AMPK* gamma (Fig. 3 B and C). Sex-specific expression was also found for *CAMK4* and *SREBP1* mRNAs. Indeed, from male stage 1 to male stage 3, a 55% significant decrease was observed for the *CAMK4* mRNA level whereas no variation was observed between the female stages. For *SREBP1* mRNA level, an increase of 35% was quantified from stage 1 to stage 3 (Fig. 6 C and D).

3.4.2. mRNAs of glucose metabolism

The mRNA levels of three genes of glucose metabolism that, according to the literature, could be putative downstream targets of AMPK signaling pathway were measured. By querying the GigasDatabase, we found three ESTs that fell into this selection. These ESTs encoded the phosphatidylinositol-4,5-bisphosphate 3-kinase catalytic subunit (*PI3K*), protein kinase AKT (*AKT*) and the cAMP Responsive Element Binding protein (*CREB*).

The *PI3K* sequence (Sigenae accession number HS190998) was identified as a 693-base pair sequence. Based on blast and alignment work with characterized vertebrate pi3k sequences, this *C. gigas* cDNA sequence appeared partial, as the 5'UTR and the beginning of the coding region are missing. The stop codon was characterized and the 3'UTR region found to be 153 base pairs long. Partial *C. gigas* PI3K deduced protein is 179 amino acids long and corresponds to the 922-amino acid long PI3K *C. gigas* sequence found in the complete genome sequence (GenBank accession number EKC40180) [58]. The *AKT* sequence (Sigenae accession number FP002673) has been identified as a 794-base pair sequence in which the 3'UTR and the end of the coding region has not yet been characterized and the 5'UTR is 145 base pairs long. By blast on the oyster genome sequence, no significant result matched with our *C. gigas* akt mRNA. The partial *C. gigas* AKT deduced protein is 216 amino acids long with more than 54% similarity with the same region of *Haemaphysalis longicornis* AKT (GenBank accession number BAK26531). Lastly, the *CREB* sequence (Sigenae accession number AM859217) was identified. This complete cDNA sequence of 2,178 base pairs has a 5'UTR of 165 base pairs and a 3'UTR of 1,155 base pairs. The partial *C. gigas* CREB deduced protein is 285 amino acids long, corresponding to the *C. gigas CREB* mRNA

(100% similarity) characterized recently in the complete genome sequence of *C. gigas* (GenBank accession number EKC32156).

Gene expression of these mRNAs belonging to the glucose metabolism was assayed by real-time PCR. Between stage 0 and later stages of gametogenesis, the level of *PI3K* mRNA decreased in males, while an increase was observed in females (Fig. 7 A). *AKT* mRNA level showed a significant decrease of 56% between stages 0 and 3 in males over the course of gametogenesis, while female samples showed mRNA levels significantly lower in stages 1 and 2 than in stages 0 and 3 (Fig. 7 B).

CREB mRNA levels showed no significant difference during the gametogenesis in females, those in males were 4.62 greater in stage 3 compared to the other stages. Finally, differences between male and female mRNA relative levels were observed for *PI3K*, *AKT* and *CREB*. For *PI3K* mRNA relative level, males expressed more (average mean 100%) compared with females, regardless of the stage. *CREB* mRNA levels were significantly higher in males than in females at stages 2 and 3. For *AKT*, significant differences were observed between sexes at stages 1 and 3, in the opposite direction: a higher value in males at stage 1 and a lower value at stage 3.

3.5. Multi-variable correlations

A Spearman correlation coefficient matrix was calculated to ascertain the relationship among all the variables including thr172 phosphorylation of AMPK alpha and relative mRNA levels, using the adjusted Holm-Bonferonni correction p-value (Table 2). No significant correlations between thr172 phosphorylation of AMPK alpha and other mRNA levels were found. Looking at the relationships among mRNA, entire *AMPK* alpha mRNA appeared positively correlated with *AMPK* beta and *AMPK* gamma mRNAs (Table 2). All *AMPK* subunits mRNAs showed significant correlations with glucose metabolism-related pi3k mRNA levels. For fatty acid metabolism, entire *AMPK* alpha and *AMPK* beta mRNA levels showed a correlation with *CAMK4* mRNA levels and *NCOA4* (this latter only with *AMPK* alpha mRNA level). No significant correlations between targets of lipid and glucose metabolisms were found. While looking at correlations between these two metabolisms, positive correlations were revealed between pi3k mRNA levels and *NCOA4-CAMK4* mRNA levels (Table 2).

4. Discussion

4.1. AMPK beta and AMPK gamma mRNAs in Crassostrea gigas

In the Pacific oyster, we characterized the two non-catalytic subunits of the AMPK heterotrimer, AMPK beta and AMPK gamma, to make a complete characterization of the AMPK system with the three subunits, including the AMPK alpha previously characterized [64]. When examining the phylogenetic tree generated, the *C. gigas* AMPK beta subunit seems to be slightly closer to the AMPK beta1 group sequence. Nevertheless, in *C. gigas* AMPK beta, the serine 24/25 phosphorylation site is absent, suggesting that *C. gigas* AMPK beta is related to an AMPK beta2 subunit. Indeed, the serine 24/25 phosphorylation site is characteristic of the AMPK beta1 isoform, which is responsible for its nuclear localization [66], and this specificity is lost in the AMPK beta2 isoform [43, 72]. Several other specific phosphorylation sites [43, 66, 73] have been characterized in *C. gigas* AMPK beta. The determinant serine 108 phosphorylation site, required for the activation of the AMPK enzyme [66] appeared conserved and positioned at serine 102 in *C. gigas*. The serine 182 phosphorylation site is also conserved. Serine 182 probably regulates the localization of the subunit but has no effect on AMPK kinase activity [66]. Neither serine 96 nor serine 101 is conserved in the *C. gigas* AMPK beta subunit.

Examining the phylogenetic tree generated, the *C. gigas* AMPK gamma subunit seems to be slightly closer to the AMPK gamma2 group sequence. In *C. gigas*, AMPK gamma contained the 4-tandem-repeat cystathionine beta-synthase (CBS) motif (termed Bateman) [71]. CBS domains are known to

regulate the activity of AMPK in response to binding molecules with adenosyl groups such as AMP or ATP [74], and therefore constitute important domains for the functionality of the AMPK system.

4.2. AMPK functioning in the gonad during gametogenesis

In *C. gigas,* both the entire AMPK alpha (62 kDa) and the truncated AMPK alpha (45 kDa) were already detected in some tissues [64]. The amount of truncated AMPK alpha was up-regulated under hypoxia in the smooth muscle and was supposed to play a role to maintain aerobic metabolism in this tissue [56]. Here we showed that the amount of truncated AMPK alpha remained unchanged during gametogenesis in both male and female gonads, and might not play a role in the control of the metabolism during reproduction in this tissue.

In our model, thr172 phosphorylation of AMPK alpha, which is highly conserved in all AMPK alpha homologues and important for activation [75, 76], was assayed in the gonad using western-blot as has been done in many other species [77-79]. We clearly showed a sex-specific amount of thr172 phosphorylation of AMPK alpha that has not previously been reported *in vivo* in other species. In oyster, AMPK might thus be a master regulator to maintain the energy available in the gonad during gametogenesis. At the mature stage of vitellogenesis in oocytes (stage 3), thr172 phosphorylation of AMPK alpha was almost completely inhibited in the gonad partially due to the significant decrease in the total amount of entire AMPK alpha (62 kDa). By calculating the ratio between thr172 phosphorylation of AMPK alpha and entire AMPK alpha (62 kDa), we can conclude that there is almost 3.5 fold decrease in the phosphorylation level of AMPK alpha thr172 residue in the female gonad when comparing stage 2 to stage 3.

Only one study has previously reported a sexual dimorphism of AMPK activation, which was reported in human muscle, and suggested to be due to the sex-specific muscle morphology reported in women: a higher proportion of type I muscle fibers exist in women compared with men [80]. In vertebrate models, many studies report the involvement of protein AMPK activation in oocyte maturation. For example, using immunohistochemistry, AMPK alpha1 was localized in rat granulosa cells, corpus luteum, oocytes and, less abundantly, in theca cells [79]. In cell culture, thr172 phosphorylation of AMPK alpha using pharmacological compounds 5-amino-1- beta-D-ribofuranosyl-imidazole-4-carboxamide (AICAR) stimulates and accelerates the germinal vesicle breakdown (GVBD) of the mouse oocyte [81-83]. Conversely, pharmacologically stimulated AMPK reduces the steroid hormone progesterone secretion in rat granulosa cells [79], and AMPK agonist blocked sea-water induced GVBD in a marine worm [84]. In these models, since no data could be obtained in the *in vivo* activation of AMPK during oogenesis, the question was not resolved of whether AMPK played a role during cytoplasmic maturation of oocytes or only in germinal vesicle breakdown (GVBD) [38]. In oyster, since AMPK alpha expression and phosphorylation is almost totally shutdown in stage 3 of gametogenesis in females, AMPK probably does not play a role in cytoplasmic maturation of oocytes. Vitellogenesis requires full synthesis of glucose and fatty acid reserves into oocytes [76], and might be incompatible with an active AMPK signaling pathway that switches off ATP-consuming anabolic pathways [39]. Pacific oysters have external fertilization and release their gametes into seawater where prophase-arrested oocytes reinitiate meiosis, undergo GVBD, and proceed to metaphase I, where they are arrested again until fertilization [85]. Taken together, our results show that AMPK activation might not be necessary for vitellogenesis in oyster but rather for later GVBD, which was not assayed here. Further analysis will be necessary to determine whether AMPK is activated or not and, therefore, whether it is important for GVBD in mature oocytes in oysters.

In male gonads, thr172 phosphorylation of AMPK alpha was observed at a constant level from stage 1 to stage 3, suggesting that it is important in the production, differentiation and maturation processes of spermatozoids. AMPK plays central role in the maintenance of cell energy levels by regulating among other pathway the glycolysis. In vertebrates, spermatozoa motility and capacitation are directly dependent on ATP supply that is generated mainly by glycolysis or by mitochondrial activity in this cell-type [86]. In boar, AMPK plays an important and necessary

regulatory role in the spermatozoa function [87, 88]. Moreover, major defects in male fertility were observed in transgenic male mice lacking *AMPK* alpha [89]☐ spermatozoa had structural abnormalities and were less motile than in control mice, associated with a 50% decrease in mitochondrial activity and a 60% decrease in basal oxygen consumption [89]. Similarly in oyster, we can make the hypothesis that AMPK activation in spermatozoa might control glycolysis to maintain ATP available for motility regulation. The origin of the constant thr172 phosphorylation of AMPK alpha in male oysters could be linked with a specific expression of liver kinase B1 (LKB1), the master upstream kinase for the AMPK threonine 172 phosphorylation site [73, 90]. Indeed, a short isoform of LKB1 specifically expressed in the testis was reported to play a major role for sperm maturation in mice [91]. Mice lacking LKB1 revealed a near complete absence of mature spermatozoa, and spermatids were completely non-motile and displayed abnormal acrosome morphology [91]. In male oysters, the long-term thr172 phosphorylation of AMPK alpha during gametogenesis could induce mitochondrial biogenesis and up-regulation of mitochondrial enzyme content, as already reported after long-term activation of AMPK in skeletal muscles of mouse [92]. Indeed, in vertebrates, chronic activation of AMPK promotes mitochondrial biogenesis and expression of nuclear-encoded mitochondrial genes by up-regulating peroxisome proliferator-activated receptor gamma coactivator 1-alpha (PGC-1 alpha) [93].

In this study, we demonstrated sex-specific variation of *AMPK* subunit mRNA expression. *AMPK* alpha was over-expressed in males during the first stages of gametogenesis when mitotic activity and differentiation of germinal cells occurred. Moreover, at all stages of gametogenesis mRNA of all subunits, *AMPK* alpha, beta and gamma, were up-regulated in males relative to females. These sex-dependent mRNA levels could be due to different balances between the processes of translation and mRNA degradation between males and females. Indeed, the regulation of mRNA degradation has a central role in the control of gene expression [94-96] and degradation of mRNA has been shown to be linked with processing bodies (P-bodies) and related granules [97]. P-bodies and related granules, known as "male germ granules" and "maternal mRNA storage granules", have been observed in different organisms such as mammals and yeasts [97]. P-bodies and granules both accumulate a fraction of translationally silent mRNAs and thus could be defined as sites of mRNA storage, reversible mRNA repression and mRNA degradation [97, 98].

4.3. Regulation of the AMPK system during gametogenesis

AMPK effects are known to be mediated both by short-term phosphorylation of downstream regulatory proteins, to stimulate catabolic processes and inhibit anabolic processes, and by long-term activation on gene expression [93, 99, 100]. The partial or complete mRNA sequences of seven AMPK-related targets (*ACC, NCOA4, CAMK4, SREBP1, PI3K, AKT, CREB*) were obtained by bioinformatic data mining in available *C. gigas* genomic databases (especially Sigenae.org) and were confirmed or completed, when partial, using the complete genome sequence that was very recently published [58]. We analyzed during gametogenesis of oysters the link between the thr172 phosphorylation of AMPK alpha and mRNA abundance of different targets belonging to glucose and lipid metabolism. No significant correlation was found using the strict Holm-Bonferonni correction. We can therefore conclude that mRNA expression of these targets is not directly regulated by AMPK activation. However, we demonstrated that the mRNA levels of entire *AMPK* alpha, beta and gamma showed positive correlation with mRNA levels of three main targets: two targets of fatty acid oxidation (camk4 and ncoa4), and one of glucose metabolism (pi3k). This could indicate a common regulation of mRNA expression of these genes during gametogenesis and, therefore, a common master regulator that remains to be discovered.

In the gonad, *CAMK4* mRNA levels are up-regulated during early stages of gametogenesis, such as early mitosis. The calcium/calmodulin-dependent protein kinase type IV (CAMK4) is a kinase that has a limited tissue distribution (lymphocytes, neurons and male germ cells). The activating factors of CAMK4 are not yet clear, however, a lack of CAMK4 protein expression is responsible for infertility in males of various species. In mouse, CAMK4 is expressed in male germ cells and spermatids and has been implicated in the control of the differentiation of germ cells into mature

spermatozoa [101]. In *C. gigas*, comparing sex-specific mRNA levels, *NCOA4* seems to be more expressed in male development, and mainly during maturation stages. NCOA4 encodes an androgen receptor coactivator and may interact with androgen receptor-like in a ligand-dependent manner. In mouse, NCOA4 protein has been detected in male and female reproductive tissues and also in oocytes [102, 103]. NCOA4 has been characterized to interact and enhances the transcriptional activity of multiple ligand-activated nuclear receptors, like the androgen receptor (AR), estrogen and progesterone [102, 104, 105]. Fatty acid metabolism, reflected by NCOA4 and CAMK4 and glucose metabolism through master kinase PI3K, could represent the energy network that supports gametogenesis in oyster, as already suggested by several studies in which different key targets of insulin pathway were characterized in reproductive tissues [16-18].

4.4. Suggested roles of CREB, PI3K, and AKT in oyster reproduction

Some targets that we selected as linked with the AMPK pathway did not show any correlation with AMPK activation, but showed stage and/or sex-specific mRNA levels during gametogenesis in oyster. In *C. gigas*, *CREB* mRNA levels showed a significant increased expression in males during the late stage of gametogenesis. The glucose metabolism-related transcription factor CREB has been described to be involved in gluconeogenesis, and regulates the growth of oocytes and sperm [106, 107]. Activated CREB has been shown to be essential for maintaining spermatogenesis in Sertoli cells [108] and CREB positively auto-regulates its own expression by binding to a CRE-like element in its promoter [109]. In the freshwater hydrozoan hydra, CREB has been shown to play a role in promeiotic or meiotic stages [110], but no involvement during maturation stages has been clearly identified.

The protein kinase AKT, the major downstream target of PI3K, has been characterized in oocytes and sperm of several species [111-113]. *AKT* mRNA levels might be more important during the resting stage, when early mitosis can occur, and for males at stage 1. Lee et al. (2007) [112] showed that the PI3K-Akt pathway plays a central role in the self-renewal of spermatogonial stem cells and also plays important roles in differentiating spermatogonia. In *C. gigas*, we can hypothesize that AKT helps the early mitotic proliferation that occurs at the end of the sexual resting stage. In *C. gigas* females at stage 3, compared with males and other stages, a significant increase of *AKT* mRNA levels was demonstrated. This observation supports the hypothesis that glucose metabolism is involved in vitellogenesis and/or in late maturation stage in oyster, as demonstrated in vertebrates and fishes [114, 115]

4.5. Conclusion

The Bateman principle shows that, in many species, eggs are much larger than sperm. Sperm are thus often considered energetically cheaper to produce than eggs [116-118]. However, this principle does not seem to be true for species that reproduce by spawning, where the investment made by each sex can be considered approximately equal [119]. During gametogenesis, oysters produce a greater number of gametes per male than per female. This difference of quantity occurs during mitosis, when germ cells divide massively to start gamete production. The stage 1 differences seen between male and female mRNA levels of *PI3K*, *AKT* and *NCOA4*, suggest that these targets might be necessary to support the massive germ cell division observed during mitosis.

AMPK was sex-specifically regulated depending on gender in the gonad of *C. gigas*. AMPK activation was constant for male gametogenesis and was disrupted during vitellogenesis in females. Recent advances in gamete signaling pathways revealed that AMPK is involved in gamete quality of *Sus scorfa* [120]. A high individual variability of gamete quality was reported in *C. gigas* [121, 122] and it would be interesting to test whether AMPK signaling could play a role in gamete quality in our model. Looking more deeply into the energy network described by the Spearman correlation coefficient matrix, we can say that network organization with gene clusters can be drawn for managing the energy during the energy spending period of *C. gigas* gametogenesis. The importance of AMPK and different mRNA targets that have been characterized as being potentially

involved in *C. gigas* reproduction could be assessed by developing functional in vivo studies in order to disrupt or enhance the metabolic pathways by using pharmacological stimulation with the AMPK inhibitor AICAR [123] or RNA interference disruption technology recently developed in oyster [65, 124].

Acknowledgements

References

1.	Pauley GB, Van Der Raay B, Troutt D. Species profiles: life histories and environmental requirements of coastal fishes and invertebrates (Pacific Northwest) - Pacific oyster. United States Fish Wildlife Service. Biological Report 1988; 82:28.
2.	Amemiya I. On the sex-change of the Japanese common oyster, *Ostrea gigas* Thunberg. Proceedings of the Imperial Academy (of Japan) 1929; 5:284-286.
3.	Fabioux C, Huvet A, Le Souchu P, Le Pennec M, Pouvreau S. Temperature and photoperiod drive *Crassostrea gigas* reproductive internal clock. Aquaculture 2005; 250:458-470.
4.	Fabioux C, Huvet A, Lelong C, Robert R, Pouvreau S, Daniel J-Y, Minguant C, Le Pennec M. Oyster vasa-like gene as a marker of the germline cell development in *Crassostrea gigas*. Biochemical and biophysical research communications 2004; 320:592-598.
5.	Fabioux C, Pouvreau S, Le Roux F, Huvet A. The oyster vasa-like gene: a specific marker of the germline in *Crassostrea gigas*. Biochemical and biophysical research communications 2004; 315:897-904.
6.	Enríquez-Díaz M, Pouvreau S, Chávez-Villalba J, Pennec M. Gametogenesis, reproductive investment, and spawning behavior of the Pacific giant oyster *Crassostrea gigas*: evidence of an environment-dependent strategy. Aquaculture International 2009; 17:491-506.
7.	Franco A, Heude Berthelin C, Goux D, Sourdaine P, Mathieu M. Fine structure of the early stages of spermatogenesis in the Pacific oyster, *Crassostrea gigas* (Mollusca, Bivalvia). Tissue & cell 2008; 40:251-260.
8.	Franco A, Jouaux A, Mathieu M, Sourdaine P, Lelong C, Kellner K, Berthelin CH. Proliferating cell nuclear antigen in gonad and associated storage tissue of the Pacific oyster *Crassostrea gigas*: seasonal immunodetection and expression in laser microdissected tissues. Cell and Tissue Research 2010; 340:201-210.
9.	Berthelin CH, Laisney J, Espinosa J, Martin O, Hernandez G, Mathieu M, Kellner K. Storage and reproductive strategy in *Crassostrea gigas* from two different growing areas (Normandy and the Atlantic coast, France). Invertebrate Reproduction & Development 2001; 40:79-86.
10.	Dridi S, Romdhane MS, Elcafsi Mh. Seasonal variation in weight and biochemical composition of the Pacific oyster, *Crassostrea gigas* in relation to the gametogenic cycle and environmental conditions of the Bizert lagoon, Tunisia. Aquaculture 2007; 263:238-248.
11.	Berthelin CH, Kellner K, Mathieu M. Storage metabolism in the Pacific oyster (*Crassostrea gigas*) in relation to summer mortalities and reproductive cycle (west coast of France). Comparative Biochemistry and Physiology Part B: Biochemistry and molecular biology 2000; 125:359-369.

12.   Bigot L, Zatylny-Gaudin C, Rodet F, Bernay B, Boudry P, Favrel P. Characterization of GnRH-related peptides from the Pacific oyster *Crassostrea gigas*. Peptides 2012; 34:303-310.

13.   Lafore J. Analyse spatio-temporelle de l'expression du gène codant pour le récepteur du neuropeptide Y, identifié pour son différentiel d'expression entre des lignées d'huîtres Résistantes et Sensibles à la mortalité estivale. In. Paris: Université Pierre et Marie Curie; 2008: 24.

14.   Matsumoto T, Nakamura AM, Mori K, Kayano T. Molecular characterization of a cDNA encoding putative vitellogenin from the Pacific oyster *Crassostrea gigas*. Zoological science 2003; 20:37-42.

15.   Matsumoto T, Nakamura AM, Mori K, Akiyama I, Hirose H, Takahashi Y. Oyster estrogen receptor: cDNA cloning and immunolocalization. General and Comparative Endocrinology 2007; 151:195-201.

16.   Hamano K, Awaji M, Usuki H. cDNA structure of an insulin-related peptide in the Pacific oyster and seasonal changes in the gene expression. The Journal of endocrinology 2005; 187:55-67.

17.   Gricourt L, Bonnec G, Boujard D, Mathieu M, Kellner K. Insulin-like system and growth regulation in the Pacific oyster *Crassostrea gigas*: hrIGF-1 effect on protein synthesis of mantle edge cells and expression of an homologous insulin receptor-related receptor. General and Comparative Endocrinology 2003; 134:44-56.

18.   Jouaux A, Franco A, Heude-Berthelin C, Sourdaine P, Blin JL, Mathieu M, Kellner K. Identification of Ras, Pten and p70S6K homologs in the Pacific oyster *Crassostrea gigas* and diet control of insulin pathway. General and Comparative Endocrinology 2011; 176:28-38.

19.   Galtsoff PS. The role of chemical stimulation in the spawning reactions of *Ostrea Virginica* and *Ostrea Gigas*. Proceedings of the National Academy of Sciences of the United States of America 1930; 16:555-559.

20.   Royer J, Seguineau C, Park KI, Pouvreau S, Choi KS, Costil K. Gametogenetic cycle and reproductive effort assessed by two methods in 3 age classes of Pacific oysters, *Crassostrea gigas*, reared in Normandy. Aquaculture 2008; 277:313-320.

21.   van der Veer HW, Cardoso JFMF, van der Meer J. The estimation of DEB parameters for various Northeast Atlantic bivalve species. Journal of Sea Research 2006; 56:107-124.

22.   Soletchnik P, Razet D, Geairon P, Faury N, Goulletquer P. Ecophysiology of maturation and spawning in oyster (*Crassostrea gigas*): Metabolic (respiration) and feeding (clearance and absorption rates) responses at different maturation stages. Aquatic Living Resources 1997; 10:177-185.

23.   Ernande B, Clobert J, McCombie H, Boudry P. Genetic polymorphism and trade-offs in the early life-history strategy of the Pacific oyster, *Crassostrea gigas* (Thunberg, 1795): a quantitative genetic study. Journal of Evolutionary Biology 2003; 16:399-414.

24.   Huvet A, Normand J, Fleury E, Quillien V, Fabioux C, Boudry P. Reproductive effort of Pacific oysters: A trait associated with susceptibility to summer mortality. Aquaculture 2010; 304:95-99.

25.   Pernet F, Barret J, Gall PL, Corporeau C, Dégremont L, Lagarde F, Pépin JF, Keck N. Mass mortalities of Pacific oysters *Crassostrea gigas* reflect infectious diseases and vary with farming practises in the Thau lagoon. Aquaculture Environement Interactions 2012; Vol. 2:215–237.

26.   Samain JF, Degremont L, Soletchnik P, Haure J, Bedier E, Ropert M, Moal J, Huvet A, Bacca H, Van Wormhoudt A, Delaporte M, Costil K, et al. Genetically based resistance to summer mortality in the Pacific oyster (*Crassostrea gigas*) and its relationship with physiological, immunological characteristics and infection processes. Aquaculture 2007; 268:227-243.

27.   Soletchnik P, Le Moine O, Faury N, Razet D, Geairon P, Goulletquer P. Summer mortality of the oyster in the Bay Marennes-Oleron: Spatial variability of environment and biology using a geographical information system (GIS). Aquatic Living Resources 1999; 12:131-143.

28.   Schneider JE. Energy balance and reproduction. Physiology & behavior 2004; 81:289-317.

29. Wade GN, Jones JE. Neuroendocrinology of nutritional infertility. American journal of physiology. Regulatory, integrative and comparative physiology 2004; 287:1277-1296.

30. Naimi A, Martinez AS, Specq ML, Diss B, Mathieu M, Sourdaine P. Molecular cloning and gene expression of Cg-Foxl2 during the development and the adult gametogenetic cycle in the oyster *Crassostrea gigas*. Comparative Biochemistry and Physiology Part B: Biochemistry and molecular biology 2009; 154:134-142.

31. Santerre C, Sourdaine P, Martinez AS. Expression of a natural antisense transcript of Cg-Foxl2 during the gonadic differentiation of the oyster *Crassostrea gigas*: first demonstration in the gonads of a lophotrochozoa species. Sexual development 2012; 6:210-221.

32. Naimi A, Martinez AS, Specq ML, Mrac A, Diss B, Mathieu M, Sourdaine P. Identification and expression of a factor of the DM family in the oyster *Crassostrea gigas*. Comparative Biochemistry and Physiology Part A: Molecular Integrative Physiology 2009; 152:189-196.

33. Fleury E, Fabioux C, Lelong C, Favrel P, Huvet A. Characterization of a gonad-specific transforming growth factor-β superfamily member differentially expressed during the reproductive cycle of the oyster *Crassostrea gigas*. Gene 2008; 410:187-196.

34. Corporeau C, Groisillier A, Jeudy A, Barbeyron T, Fleury E, Fabioux C, Czjzek M, Huvet A. A functional study of transforming growth factor-beta from the gonad of Pacific oyster *Crassostrea gigas*. Marine Biotechnology 2011; 13:971-980.

35. Dheilly N, Lelong C, Huvet A, Kellner K, Dubos MP, Riviere G, Boudry P, Favrel P. Gametogenesis in the Pacific oyster *Crassostrea gigas*: a microarrays-based analysis identifies sex and stage specific genes. PLoS One 2012; 7:36353.

36. Bacca H, Huvet A, Fabioux C, Daniel J-Y, Delaporte M, Pouvreau S, Van Wormhoudt A, Moal J. Molecular cloning and seasonal expression of oyster glycogen phosphorylase and glycogen synthase genes. Comparative Biochemistry and Physiology Part B: Biochemistry and molecular biology 2005; 140:635-646.

37. Tosca L, Dupont J. Un role de la kinase activé par l'AMP (AMPK) dans le métabolisme et la reproduction. Regard sur la Biochimie 2007.

38. Tosca L, Chabrolle C, Dupont J. AMPK: a link between metabolism and reproduction? Medecine sciences 2008; 24:297-300.

39. Hardie DG. Management of cellular energy by the AMP-activated protein kinase system. FEBS letters 2003; 546:113-120.

40. Kemp BE, Stapleton D, Campbell DJ, Chen ZP, Murthy S, Walter M, Gupta A, Adams JJ, Katsis F, van Denderen B, Jennings IG, Iseli T, et al. AMP-activated protein kinase, super metabolic regulator. Biochemical Society Transactions 2003; 31:162-168.

41. Dyck JR, Gao G, Widmer J, Stapleton D, Fernandez CS, Kemp BE, Witters LA. Regulation of 5'-AMP-activated protein kinase activity by the noncatalytic beta and gamma subunits. The Journal of biological chemistry 1996; 271:17798-17803.

42. Hawley SA, Davison M, Woods A, Davies SP, Beri RK, Carling D, Hardie DG. Characterization of the AMP-activated protein kinase kinase from rat liver and identification of threonine 172 as the major site at which it phosphorylates AMP-activated protein kinase. The Journal of biological chemistry 1996; 271:27879-27887.

43. Mitchelhill KI, Michell BJ, House CM, Stapleton D, Dyck J, Gamble J, Ullrich C, Witters LA, Kemp BE. Posttranslational modifications of the 5'-AMP-activated protein kinase beta1 subunit. The Journal of biological chemistry 1997; 272:24475-24479.

44. Woods A, Vertommen D, Neumann D, Turk R, Bayliss J, Schlattner U, Wallimann T, Carling D, Rider MH. Identification of phosphorylation sites in AMP-activated protein kinase (AMPK) for upstream AMPK kinases and study of their roles by site-directed mutagenesis. The Journal of biological chemistry 2003; 278:28434-28442.

45. Neumann D. Mammalian AMP-activated protein kinase: functional, heterotrimeric complexes by co-expression of subunits in Escherichia coli. Protein Expression and Purification 2003; 30:230-237.

46. Suter M, Riek U, Tuerk R, Schlattner U, Wallimann T, Neumann D. Dissecting the role of 5'-AMP for allosteric stimulation, activation, and deactivation of AMP-activated protein kinase. The Journal of biological chemistry 2006; 281:32207-32216.

47. Choi SL, Kim SJ, Lee KT, Kim J, Mu J, Birnbaum MJ, Soo Kim S, Ha J. The regulation of AMP-activated protein kinase by H_2O_2. Biochemical and biophysical research communications 2001; 287:92-97.

48. Hardie DG. The AMP-activated protein kinase pathway - new players upstream and downstream. Journal of cell science 2004; 117:5479-5487.

49. Boudry P, Dégremont L, Haffray P. The genetic basis of summer mortality in Pacific oyster spat and potential for improving survival by selective breeding in France. Summer mortality of Pacific oyster *Crassostrea gigas*, the Morest project. Edition Ifremer Quae 2008:153-196.

50. Latendresse JR, Warbrittion AR, Jonassen H, Creasy DM. Fixation of testes and eyes using a modified Davidson's fluid: Comparison with Bouin's fluid and conventional davidson's fluid. Toxicologic Pathology 2002; 30:524-533.

51. Martoja R, Martoja-Pierson M. Initiation aux techniques de l'histologie animale. Paris: Masson; 1967.

52. Steele S, Mulcahy MF. Gametogenesis of the oyster *Crassostrea gigas* in Southern Ireland. Journal of the Marine Biological Association of the United Kingdom 1999; 79:673-686.

53. Fleury E, Huvet A, Lelong C, de Lorgeril J, Boulo V, Gueguen Y, Bachere E, Tanguy A, Moraga D, Fabioux C, Lindeque P, Shaw J, et al. Generation and analysis of a 29,745 unique Expressed Sequence Tags from the Pacific oyster (*Crassostrea gigas*) assembled into a publicly accessible database: the GigasDatabase. BMC genomics 2009; 10:341.

54. Altschul SF, Madden TL, Schaffer AA, Zhang J, Zhang Z, Miller W, Lipman DJ. Gapped BLAST and PSI-BLAST: a new generation of protein database search programs. Nucleic acids research 1997; 25:3389-3402.

55. de Castro E, Sigrist CJ, Gattiker A, Bulliard V, Langendijk-Genevaux PS, Gasteiger E, Bairoch A, Hulo N. ScanProsite: detection of PROSITE signature matches and ProRule-associated functional and structural residues in proteins. Nucleic acids research 2006; 34:362-365.

56. Schultz J, Milpetz F, Bork P, Ponting CP. SMART, a simple modular architecture research tool: identification of signaling domains. Proceedings of the National Academy of Sciences of the United States of America 1998; 95:5857-5864.

57. Gasteiger E, Gattiker A, Hoogland C, Ivanyi I, Appel RD, Bairoch A. ExPASy: The proteomics server for in-depth protein knowledge and analysis. Nucleic acids research 2003; 31:3784-3788.

58. Zhang G, Fang X, Guo X, Li L, Luo R, Xu F, Yang P, Zhang L, Wang X, Qi H, Xiong Z, Que H, et al. The oyster genome reveals stress adaptation and complexity of shell formation. Nature 2012; 490:49-54.

59. Combet C, Blanchet C, Geourjon C, Deleage G. NPS@: network protein sequence analysis. Trends in Biochemical Sciences 2000; 25:147-150.

60. Huvet A, Herpin A, Degremont L, Labreuche Y, Samain J-F, Cunningham C. The identification of genes from the oyster *Crassostrea gigas* that are differentially expressed in progeny exhibiting opposed susceptibility to summer mortality. Gene 2004; 343:211-220.

61. Pfaffl MW. A new mathematical model for relative quantification in real-time RT-PCR. Nucleic acids research 2001; 29:45.

62. Rozen S, Skaletsky H. Primer3 on the WWW for general users and for biologist programmers. Methods in molecular biology 2000; 132:365-386.

63. Le Foll C, Corporeau C, Le Guen V, Gouygou JP, Berge JP, Delarue J. Long-chain n-3 polyunsaturated fatty acids dissociate phosphorylation of Akt from phosphatidylinositol 3'-kinase activity in rats. American journal of physiology. Endocrinology and metabolism 2007; 292:1223-1230.

64. Guevelou E, Huvet A, Sussarellu R, Milan M, Guo X, Li L, Zhang G, Quillien V, Daniel JY, Quere C, Boudry P, Corporeau C. Regulation of a truncated isoform of AMP-activated protein kinase alpha (AMPKalpha) in response to hypoxia in the muscle of Pacific oyster Crassostrea gigas. Journal of Comparative Physiology B 2013.

65. Fabioux C, Corporeau C, Quillien V, Favrel P, Huvet A. *In vivo* RNA interference in oyster-vasa silencing inhibits germ cell development. FEBS journal 2009; 276:2566-2573.

66. Warden SM, Richardson C, O'Donnell J, Jr., Stapleton D, Kemp BE, Witters LA. Post-translational modifications of the beta-1 subunit of AMP-activated protein kinase affect enzyme activity and cellular localization. The Biochemical journal 2001; 354:275-283.

67. Polekhina G, Gupta A, Michell BJ, van Denderen B, Murthy S, Feil SC, Jennings IG, Campbell DJ, Witters LA, Parker MW, Kemp BE, Stapleton D. AMPK beta subunit targets metabolic stress sensing to glycogen. Current Biology 2003; 13:867-871.

68. Hudson ER, Pan DA, James J, Lucocq JM, Hawley SA, Green KA, Baba O, Terashima T, Hardie DG. A novel domain in AMP-activated protein kinase causes glycogen storage bodies similar to those seen in hereditary cardiac arrhythmias. Current Biology 2003; 13:861-866.

69. Iseli TJ, Walter M, van Denderen BJ, Katsis F, Witters LA, Kemp BE, Michell BJ, Stapleton D. AMP-activated protein kinase beta subunit tethers alpha and gamma subunits via its C-terminal sequence (186-270). The Journal of biological chemistry 2005; 280:13395-13400.

70. Adams J, Chen ZP, Van Denderen BJ, Morton CJ, Parker MW, Witters LA, Stapleton D, Kemp BE. Intrasteric control of AMPK via the gamma1 subunit AMP allosteric regulatory site. Protein science 2004; 13:155-165.

71. Bateman A. The structure of a domain common to archaebacteria and the homocystinuria disease protein. Trends in Biochemical Sciences 1997; 22:12-13.

72. Chen Z, Heierhorst J, Mann RJ, Mitchelhill KI, Michell BJ, Witters LA, Lynch GS, Kemp BE, Stapleton D. Expression of the AMP-activated protein kinase beta1 and beta2 subunits in skeletal muscle. FEBS letters 1999; 460:343-348.

73. Woods A, Johnstone SR, Dickerson K, Leiper FC, Fryer LG, Neumann D, Schlattner U, Wallimann T, Carlson M, Carling D. LKB1 is the upstream kinase in the AMP-activated protein kinase cascade. Current Biology 2003; 13:2004-2008.

74. Kemp BE. Bateman domains and adenosine derivatives form a binding contract. Journal of clinical investigation 2004; 113:182-184.

75. Stapleton D, Mitchelhill KI, Gao G, Widmer J, Michell BJ, Teh T, House CM, Fernandez CS, Cox T, Witters LA, Kemp BE. Mammalian AMP-activated protein kinase subfamily. The Journal of biological chemistry 1996; 271:611-614.

76. Carling D, Mayer FV, Sanders MJ, Gamblin SJ. AMP-activated protein kinase: nature's energy sensor. Nature chemical biology 2011; 7:512-518.

77. Lim CT, Lolli F, Thomas JD, Kola B, Korbonits Mr, Masayasu K, Kenji K. Chapter Seventeen - Measurement of AMP-Activated Protein Kinase Activity and Expression in Response to Ghrelin. In: Methods in Enzymology, vol. Volume 514: Academic Press; 2012: 271-287.

78. Sanders MJ, Grondin PO, Hegarty BD, Snowden MA, Carling D. Investigating the mechanism for AMP activation of the AMP-activated protein kinase cascade. The Biochemical journal 2007; 403:139-148.

79. Tosca L, Froment P, Solnais P, Ferre P, Foufelle F, Dupont J. Adenosine 5'-monophosphate-activated protein kinase regulates progesterone secretion in rat granulosa cells. Endocrinology 2005; 146:4500-4513.

80. Roepstorff C, Thiele M, Hillig T, Pilegaard H, Richter EA, Wojtaszewski JF, Kiens B. Higher skeletal muscle alpha2AMPK activation and lower energy charge and fat oxidation in men than in women during submaximal exercise. The Journal of physiology 2006; 574:125-138.

81. Downs SM, Hudson ER, Hardie DG. A potential role for AMP-activated protein kinase in meiotic induction in mouse oocytes. Developmental biology 2002; 245:200-212.

82. Chen J, Hudson E, Chi MM, Chang AS, Moley KH, Hardie DG, Downs SM. AMPK regulation of mouse oocyte meiotic resumption *in vitro*. Developmental biology 2006; 291:227-238.

83. LaRosa C, Downs SM. Stress stimulates AMP-activated protein kinase and meiotic resumption in mouse oocytes. Biology of Reproduction 2006; 74:585-592.

84. Stricker SA. Inhibition of germinal vesicle breakdown by antioxidants and the roles of signaling pathways related to nitric oxide and cGMP during meiotic resumption in oocytes of a marine worm. Reproduction 2012; 143:261-270.

85. Kyozuka K, Deguchi R, Yoshida N, Yamashita M. Change in intracellular Ca^{2+} is not involved in serotonin-induced meiosis reinitiation from the first prophase in oocytes of the marine bivalve *Crassostrea gigas*. Developmental Biology 1997; 182:33-41.

86. Williams AC, Ford WC. The role of glucose in supporting motility and capacitation in human spermatozoa. Journal of andrology 2001; 22:680-695.

87. Martin-Hidalgo D, Hurtado de Llera A, Yeste M, Gil MC, Bragado MJ, Garcia-Marin LJ. Adenosine monophosphate-activated kinase, AMPK, is involved in the maintenance of the quality of extended boar semen during long-term storage. Theriogenology 2013.

88. Hurtado de Llera A, Martin-Hidalgo D, Rodriguez-Gil JE, Gil MC, Garcia-Marin LJ, Bragado MJ. AMP-activated kinase, AMPK, is involved in the maintenance of plasma membrane organization in boar spermatozoa. Biochim Biophys Acta 2013; 1828:2143-2151.

89. Tartarin P, Guibert E, Toure A, Ouiste C, Leclerc J, Sanz N, Briere S, Dacheux J-L, Delaleu B, McNeilly JR, McNeilly AS, Brillard J-P, et al. Inactivation of AMPKalpha1 induces asthenozoospermia and alters spermatozoa morphology. Endocrinology 2012; 153:3468-3481.

90. Hawley SA, Boudeau J, Reid JL, Mustard KJ, Udd L, Makela TP, Alessi DR, Hardie DG. Complexes between the LKB1 tumor suppressor, STRAD alpha/beta and MO25 alpha/beta are upstream kinases in the AMP-activated protein kinase cascade. Journal of biology 2003; 2:28.

91. Shaw RJ. LKB1: cancer, polarity, metabolism, and now fertility. The Biochemical journal 2008; 416:1-3.

92. Zong H, Ren JM, Young LH, Pypaert M, Mu J, Birnbaum MJ, Shulman GI. AMP kinase is required for mitochondrial biogenesis in skeletal muscle in response to chronic energy deprivation. Proceedings of the National Academy of Sciences of the United States of America 2002; 99:15983-15987.

93. Hardie DG. AMP-activated protein kinase: an energy sensor that regulates all aspects of cell function. Genes & development 2011; 25:1895-1908.

94. Elkon R, Zlotorynski E, Zeller KI, Agami R. Major role for mRNA stability in shaping the kinetics of gene induction. BMC genomics 2010; 11:259.

95. Grigull J, Mnaimneh S, Pootoolal J, Robinson MD, Hughes TR. Genome-wide analysis of mRNA stability using transcription inhibitors and microarrays reveals posttranscriptional control of ribosome biogenesis factors. Molecular and cellular biology 2004; 24(12):5534-5547.

96. Wilusz CJ, Wilusz J. Bringing the role of mRNA decay in the control of gene expression into focus. Trends in genetics 2004; 20:491-497.

97. Olszewska M, Bujarski JJ, Kurpisz M. P-bodies and their functions during mRNA cell cycle: mini-review. Cell biochemistry and function 2012; 30:177-182.

98. Seydoux G, Braun RE. Pathway to totipotency: lessons from germ cells. Cell 2006; 127:891-904.

99. Viollet B, Athea Y, Mounier R, Guigas B, Zarrinpashneh E, Horman S, Lantier L, Hebrard S, Devin-Leclerc J, Beauloye C, Foretz M, Andreelli F, et al. AMPK: Lessons from transgenic and knockout animals. Frontiers in bioscience : a journal and virtual library 2009; 14:19-44.

100. Ramamurthy S, Ronnett G. AMP-Activated Protein Kinase (AMPK) and Energy-Sensing in the Brain. Experimental neurobiology 2012; 21:52-60.

101. Blaeser F, Toppari J, Heikinheimo M, Yan W, Wallace M, Ho N, Chatila TA. CaMKIV/Gr is dispensable for spermatogenesis and CREM-regulated transcription in male germ cells. American journal of physiology. Endocrinology and metabolism 2001; 281:931-937.

102. Kollara A, Brown TJ. Variable expression of nuclear receptor coactivator 4 (NcoA4) during mouse embryonic development. The journal of histochemistry and cytochemistry 2010; 58:595-609.

103. Stanton JL, Green DPL. A set of 840 mouse oocyte genes with well-matched human homologues. Molecular Human Reproduction 2001; 7:521-543.

104. Yeh S, Chang C. Cloning and characterization of a specific coactivator, ARA70, for the androgen receptor in human prostate cells. Proceedings of the National Academy of Sciences of the United States of America 1996; 93:5517-5521.

105. Evangelou A, Jindal SK, Brown TJ, Letarte M. Down-regulation of transforming growth factor beta receptors by androgen in ovarian cancer cells. Cancer research 2000; 60:929-935.

106. Kwok RP, Liu XT, Smith GD. Distribution of co-activators CBP and p300 during mouse oocyte and embryo development. Molecular reproduction and development 2006; 73:885-894.

107. Waeber G, Meyer TE, LeSieur M, Hermann HL, Gerard N, Habener JF. Developmental stage-specific expression of cyclic adenosine 3',5'-monophosphate response element-binding protein CREB during spermatogenesis involves alternative exon splicing. Molecular endocrinology 1991; 5:1418-1430.

108. Walker WH. Non-classical actions of testosterone and spermatogenesis. Philosophical transactions of the Royal Society of London. Series B, Biological sciences 2010; 365:1557-1569.

109. Don J, Stelzer G. The expanding family of CREB/CREM transcription factors that are involved with spermatogenesis. Molecular and cellular endocrinology 2002; 187:115-124.

110. Chera S, Kaloulis K, Galliot B. The cAMP response element binding protein (CREB) as an integrative HUB selector in metazoans: clues from the hydra model system. Biosystems 2007; 87:191-203.

111. Andersen CB, Roth RA, Conti M. Protein kinase B/Akt induces resumption of meiosis in Xenopus oocytes. The Journal of biological chemistry 1998; 273:18705-18708.

112. Lee J, Kanatsu-Shinohara M, Inoue K, Ogonuki N, Miki H, Toyokuni S, Kimura T, Nakano T, Ogura A, Shinohara T. Akt mediates self-renewal division of mouse spermatogonial stem cells. Development 2007; 134:1853-1859.

113. Hixon ML, Boekelheide K. Expression and localization of total Akt1 and phosphorylated Akt1 in the rat seminiferous epithelium. Journal of andrology 2003; 24:891-898.

114. Cecconi S, Mauro A, Cellini V, Patacchiola F. The role of Akt signalling in the mammalian ovary. Int J Dev Biol 2012; 56:809-817.

115. Pace MC, Thomas P. Steroid-induced oocyte maturation in Atlantic croaker (*Micropogonias undulatus*) is dependent on activation of the phosphatidylinositol 3-kinase/Akt signal transduction pathway. Biology of reproduction 2005; 73:988-996.

116. Bateman AJ. Intra-sexual selection in *Drosophila*. Heredity 1948; 2:349-368.

117. Huber R, Bannasch DL, Brennan P. Aggression. Academic Press; 2011.

118. Parker GA. Why are there so many tiny sperm - Sperm competition and the maintenance of 2 Sexes. Journal of Theoretical Biology 1982; 96:281-294.

119. Don L. Does Bateman's principle apply to broadcast-spawning organisms? egg traits influence *in situ* fertilization rates among congeneric Sea Urchins. Evolution 1998; 52:1043-1056.

120. de Llera AH, Martin-Hidalgo D, Gil MC, Garcia-Marin LJ, Bragado MJ. AMP-Activated Kinase AMPK is expressed in boar spermatozoa and regulates motility. PLoS One 2012; 7:38840.

121. Corporeau C, Vanderplancke G, Boulais M, Suquet M, Quere C, Boudry P, Huvet A, Madec S. Proteomic identification of quality factors for oocytes in the Pacific oyster *Crassostrea gigas*. Journal of Proteomics 2012; 75:5554-5563.

122. Boudry P, Collet B, Cornette F, Hervouet V, Bonhomme F. High variance in reproductive success of the Pacific oyster (*Crassostrea gigas*, Thunberg) revealed by microsatellite-based parentage analysis of multifactorial crosses. Aquaculture 2002; 204:283-296.

123. Corton JM, Gillespie JG, Hawley SA, Hardie DG. 5-aminoimidazole-4-carboxamide ribonucleoside. A specific method for activating AMP-activated protein kinase in intact cells? European journal of biochemistry / FEBS 1995; 229:558-565.

124. Huvet A, Fleury E, Corporeau C, Quillien V, Daniel J-Y, Riviere G, Boudry P, Fabioux C. *In vivo* RNA interference of a gonad-specific transforming growth factor-β in the Pacific oyster *Crassostrea gigas*. Marine Biotechnology 2012; 14:402-410.

Tables

Table 1: Nucleotide sequences of *Crassostrea gigas* primers used for real-time PCR amplification.

Targets		Nucleotide sequence	Sigenae accession number	GenBank accession number	PCR efficiency (%)	Reference
AMPK alpha	sens	5'- TCCTTCTAGACAGCAGCCTCA -3'		JX104214	102	Guévélou et al., 2012
	anti-sens	5'- TTGGTGAACCACAGCTGGTA -3'				
AMPK beta	sens	5'- ACTGGCACTCGACAGCTTG -3'	CU991642, FU6OSJA01AUVKV, FU6OSJA01BDGCM		99	This study
	anti-sens	5'- CTTCTCTCCCGGTTTCCTG -3'				
AMPK gamma	sens	5'- GGAGCTGAAGGACAAACAGC - 3'	FU6OSJA01ADEEL		100	This study
	anti-sens	5' - GGAGGTGATGAGGGTCTTGA - 3'				
ACC	sens	5'- ATGGTAGCCTGGCAGATGAC - 3'	HS120730		100	This study
	anti-sens	5'- GCTGGTCTGAATGACCCAAT - 3'				
NCOA4	sens	5'- TGAGAGCATCAACAGCTTCG -3'	AM855314		99	This study
	anti-sens	5'- CATCTTGTTCAGCGTCCTCA -3'				
CAMK4	sens	5'- ATGTTGGTGGCAGTGCAG - 3'	AM856845		99	This study
	anti-sens	5'- TGGAGAGACCGAAGTCAGC - 3'				
SREBP1	sens	5'- ACAGTGCCACATCCACCAC -3'	BQ426935		100	This study
	anti-sens	5'- TGACCACCATTGTCCCAAC -3'				
PI3K	sens	5'- GACACACTTGCCCTTGACCT -3'	HS190998		100	This study
	anti-sens	5'- GGTGGACCAGCTCTTGTTCT -3'				
AKT	sens	5'- AGAAGCCCAAGCCAAACAC -3'	FP002673		99	This study
	anti-sens	5'- ATGGCAGCAATCCAGTCCT -3'				
CREB	sens	5'- CTCGCTCAGTCAGCCCATAC -3'	AM859217		100	This study
	anti-sens	5'- ACTGGTGCTACCCTGACCAC -3'				

Nucleotide code: G, guanine; C, cytosine; A, adenine; T, thymine

Table 2: Matrix of Spearman correlation coefficients among thr172 phosphorylation of AMPK alpha and mRNA relative levels of the 10 targeted genes (*AMPK* alpha, *AMPK* beta, *AMPK* gamma, *ACC*, *NCOA4*, *CAMK4*, *SREBP1*, *PI3K*, *AKT* and *CREB*) The p value is given and a "+" sign indicates a significant positive correlation with the adjusted Holm-Bonferonni correction p-value.

	AMPK alpha-T172	AMPK alpha	AMPK beta	AMPK gamma	ACC	NCOA4	CAMK4	SREBP1	PI3K	AKT	CREB
AMPK alpha-T172		0.018	0.005	0.020	0.692	0.446	0.022	0.041	0.010	0.090	0.238
AMPK alpha	*		0.000	0.000	0.012	0.001	0.001	0.605	0.000	0.204	0.004
AMPK beta	**	***		0.003	0.466	0.022	0.001	0.236	0.000	0.876	0.070
AMPK gamma	*	***	**		0.005	0.012	0.079	0.812	0.001	0.277	0.004
ACC		*		**		0.651	0.567	0.029	0.295	0.002	0.049
NCOA4		**	*	*			0.587	0.064	0.000	0.328	0.003
CAMK4	*	***	***					0.326	0.000	0.597	0.212
SREBP1	*				*				0.966	0.014	0.608
PI3K	**	***	***	***		***	***			0.243	0.043
AKT					**			*			0.179
CREB		**		**	*	**			*		

Figures

Figure 1: (A) Nucleotide and deduced amino acid sequences of *Crassostrea gigas* AMPK beta (*C. gigas_* AMPK beta-like), obtained by merging 3 contigs matching AMPK beta2 (Sigenae accession number CU991642, FU6OSJA01AUVKV and FU6OSJA01BDGCM). Black square: myristoylation site. Gray squares: serine 108 and serine 182 phosphorylation sites. Black underscore: Glycogen binding domain. Gray underscore: alpha gamma-subunit binding sequence. (B) Phylogenetic tree of AMPK beta compared to other AMPK beta subunits found in other species.
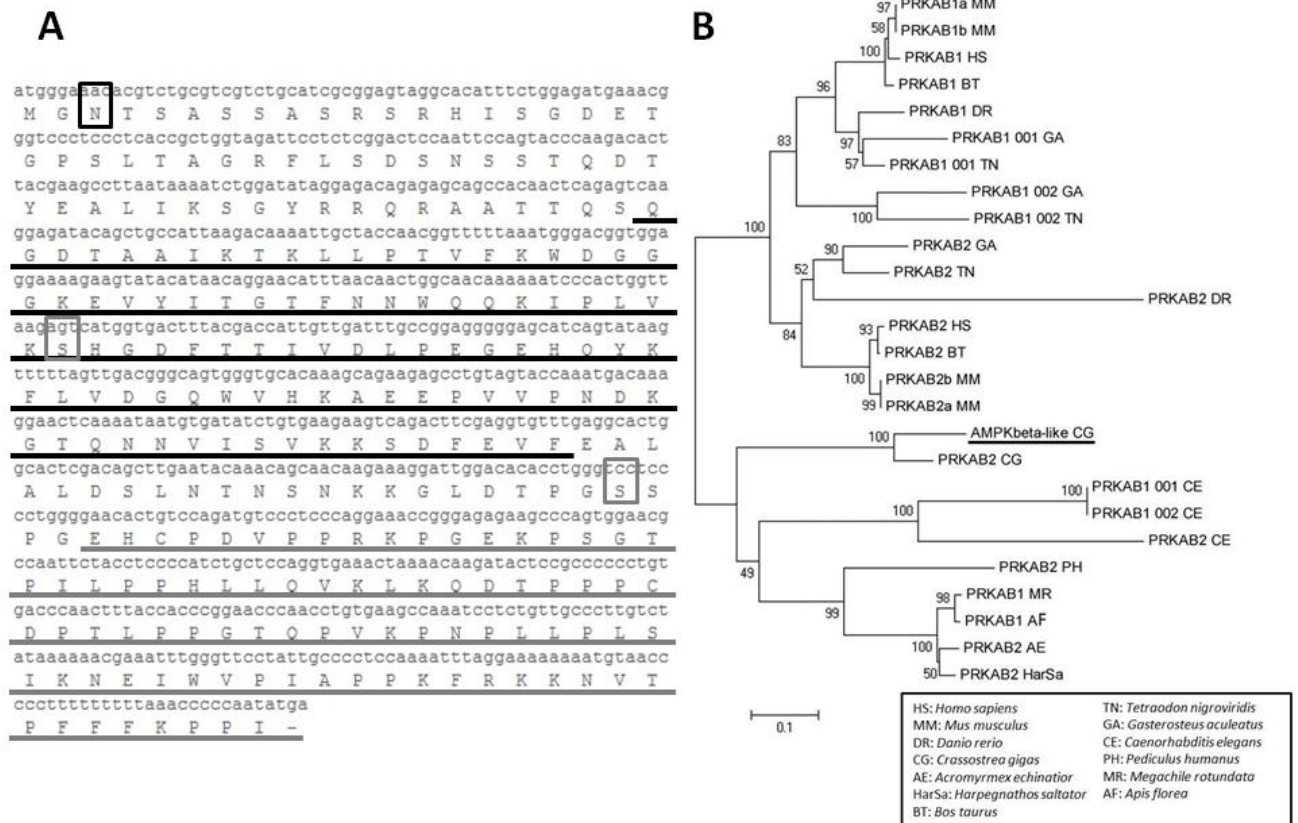
Figure 2: (A) Nucleotide and deduced amino acid alignment of *Crassostrea gigas* AMPK gamma (*C. gigas*_AMPK gamma-like; Sigenae accession number FU6OSJA01ADEEL). Black underscores: cystathionine beta-synthase motifs. (B) Phylogenetic tree of AMPK gamma-like compared to other AMPK gamma subunits found in other species.
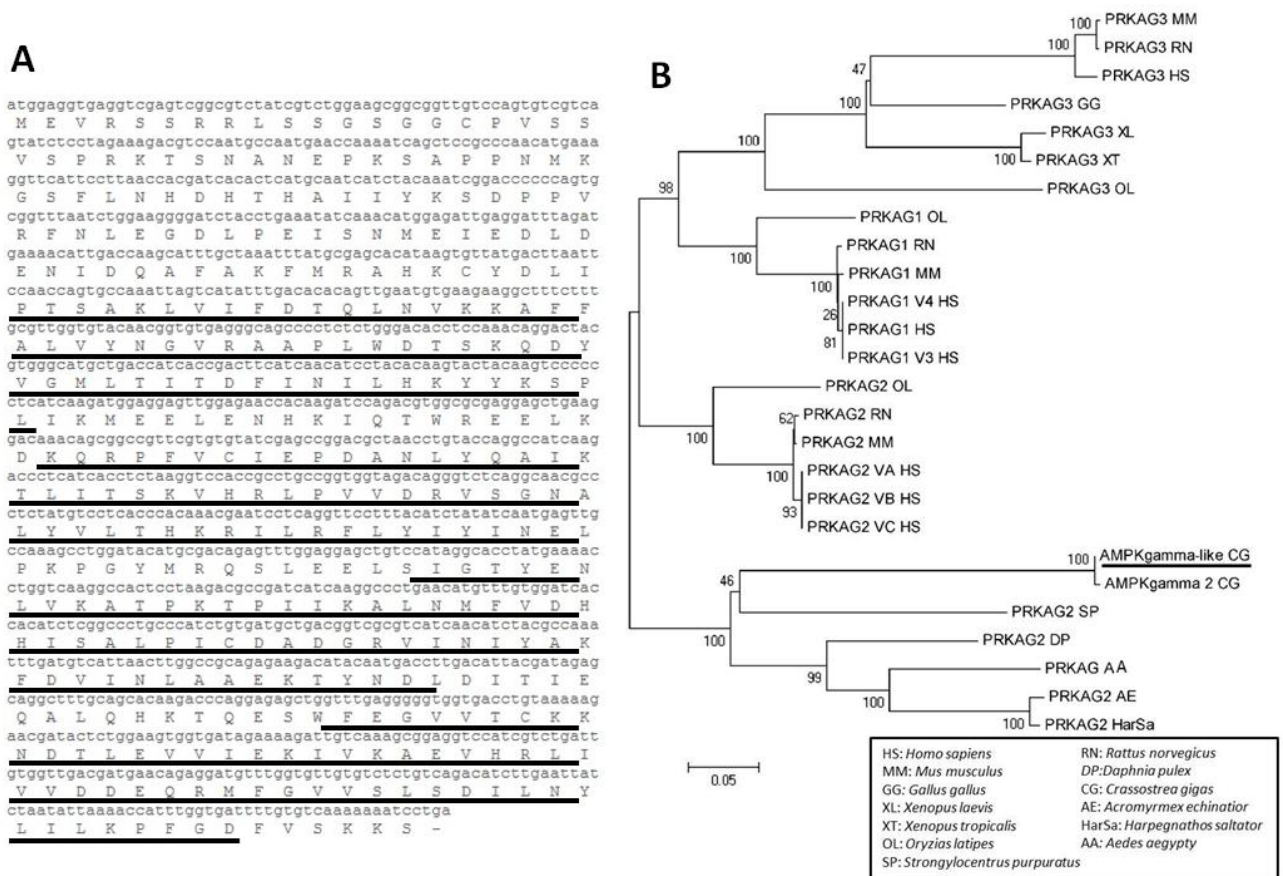
Figure 3: Relative levels of *AMPK* alpha (A), *AMPK* beta (B), and *AMPK* gamma (C) transcripts in the gonad at different reproductive stages. Results are expressed as number of copies per copy of *efl*. Gray bar: sexually undifferentiated oysters (n = 13). Black bars: males (n = 10). White bars: females (n = 10). Columns and bars show mean ± SE. Different letters indicate a significant difference between stages. Asterisks indicate a significant difference between males and females, with $p < 0.05$ (*) or $p < 0.01$ (**).
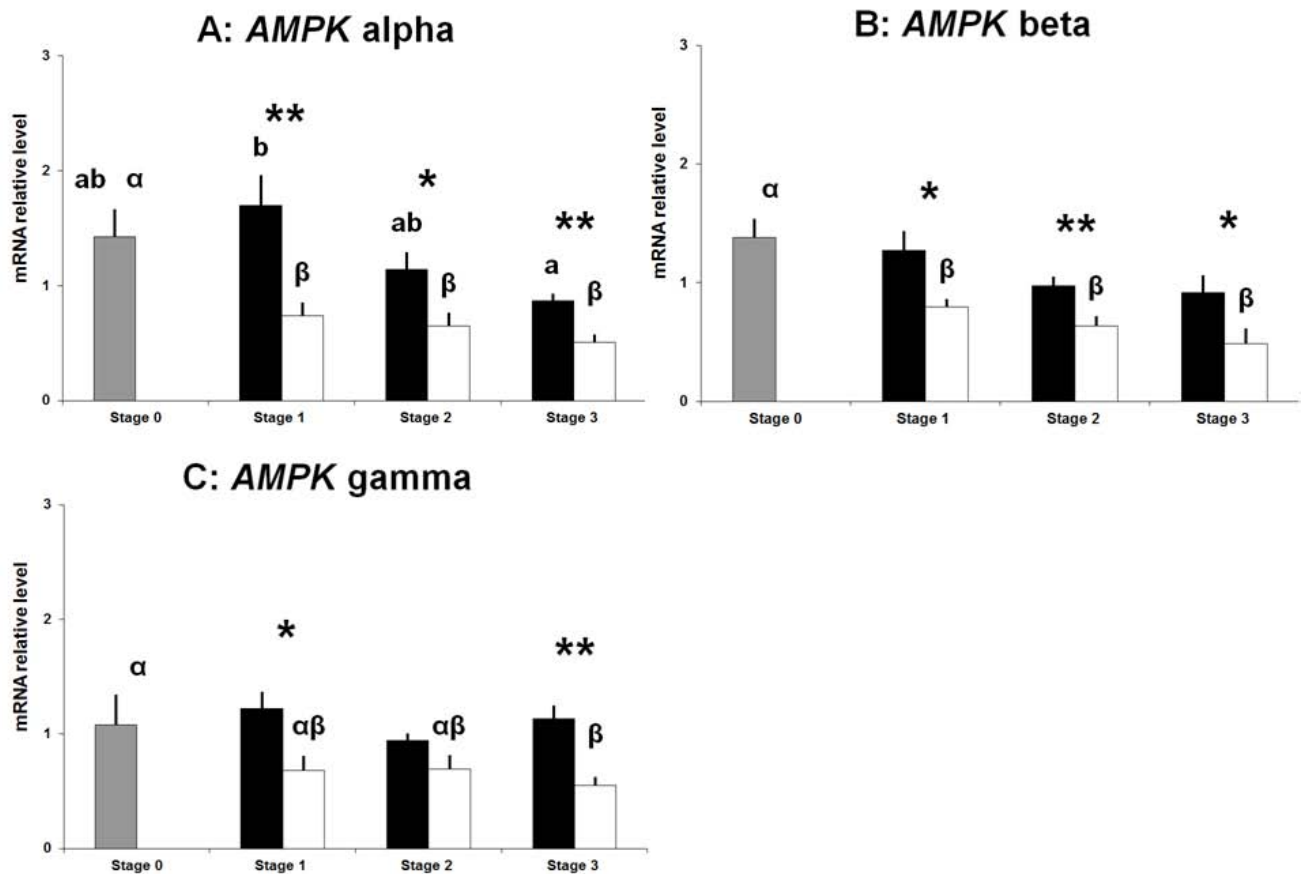
Figure 4: Western-blot of truncated AMPK alpha (45kDa) and entire AMPK alpha (62kDa) in the gonad of oysters according to sex and four different reproductive stages. (A) Representative images of truncated AMPK alpha detection at 45 kDa and histone H3 detection at 17 kDa. u: sexually undifferentiated; m: male; f: female. (B) Representative images of entire AMPK alpha detection at 62 kDa. u: sexually undifferentiated; m: male; f: female. Quantification of entire AMPK alpha (62kDa). The protein values presented on the graph were quantified on 4 western blots and expressed in relative level of OD/mm^2. Gray bar: sexually undifferentiated oysters (n = 13). Black bars: males (n = 10). White bars: females (n = 10). Columns and bars show mean ± SE. Different letters indicate a significant difference between stages. Asterisks indicate a significant difference between males and females, with $p < 0.01$ (**).
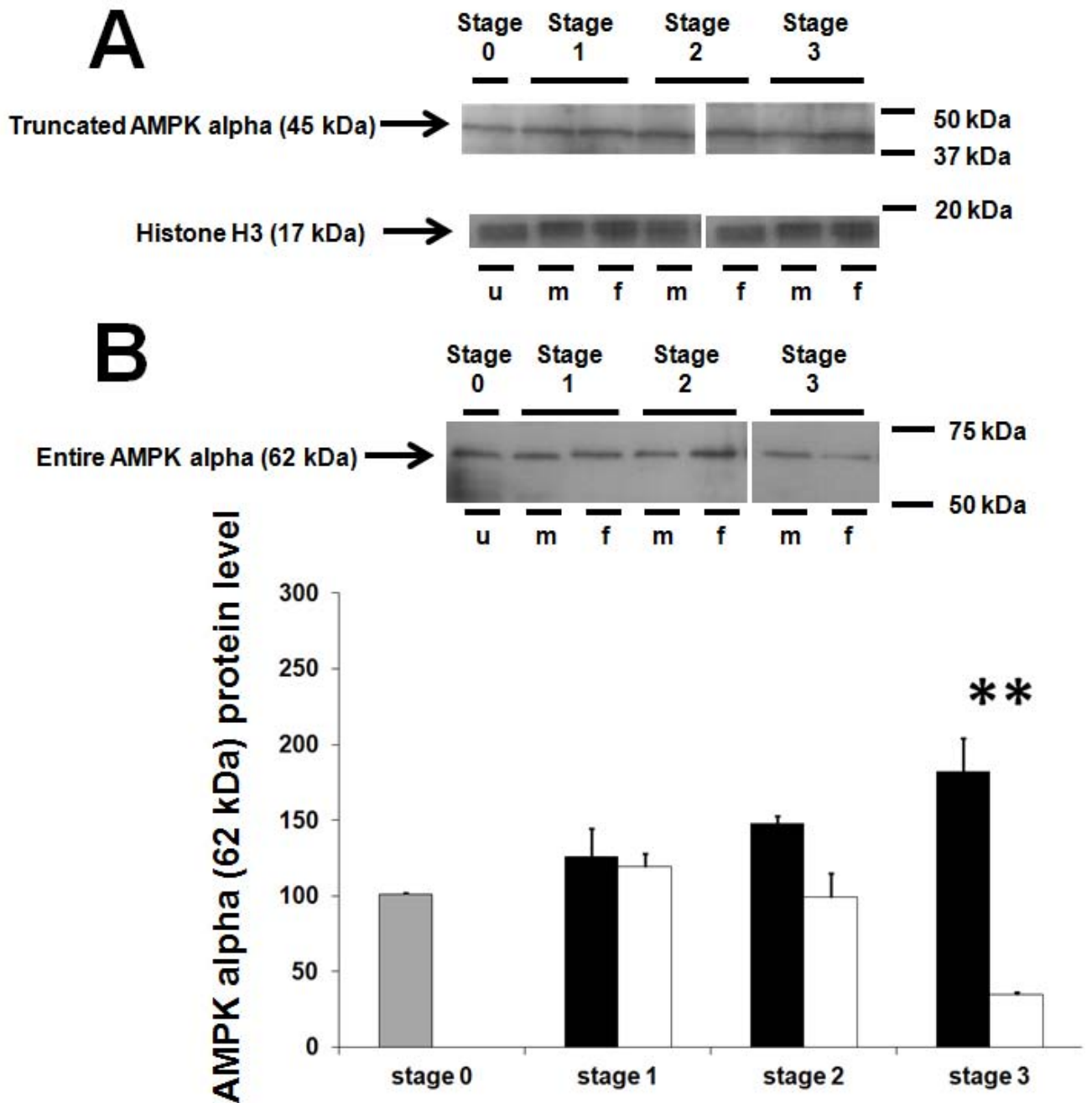
Figure 5: Western-blot of thr172 phosphorylation of AMPK alpha in the gonad of oysters according to sex and four different reproductive stages. (A) Representative images of thr172 phosphorylation of AMPK alpha detection at 62 kDa and and histone H3 detection at 17 kDa. u: sexually undifferentiated; m: male; f: female. Quantification of thr172 phosphorylation of AMPK alpha. The protein values presented on the graph were quantified on 4 western blots and expressed in relative level of OD/mm^2. (B) Ratio between the quantification of thr172 phosphorylation of AMPK alpha and entire AMPK alpha (62kDa). Gray bar: sexually undifferentiated oysters (n = 13). Black bars: males (n = 10). White bars: females (n = 10). Columns and bars show mean ± SE. Different letters indicate a significant difference between stages. Asterisks indicate a significant difference between males and females, with $p < 0.01$ (**) and $p < 0.001$ (***).
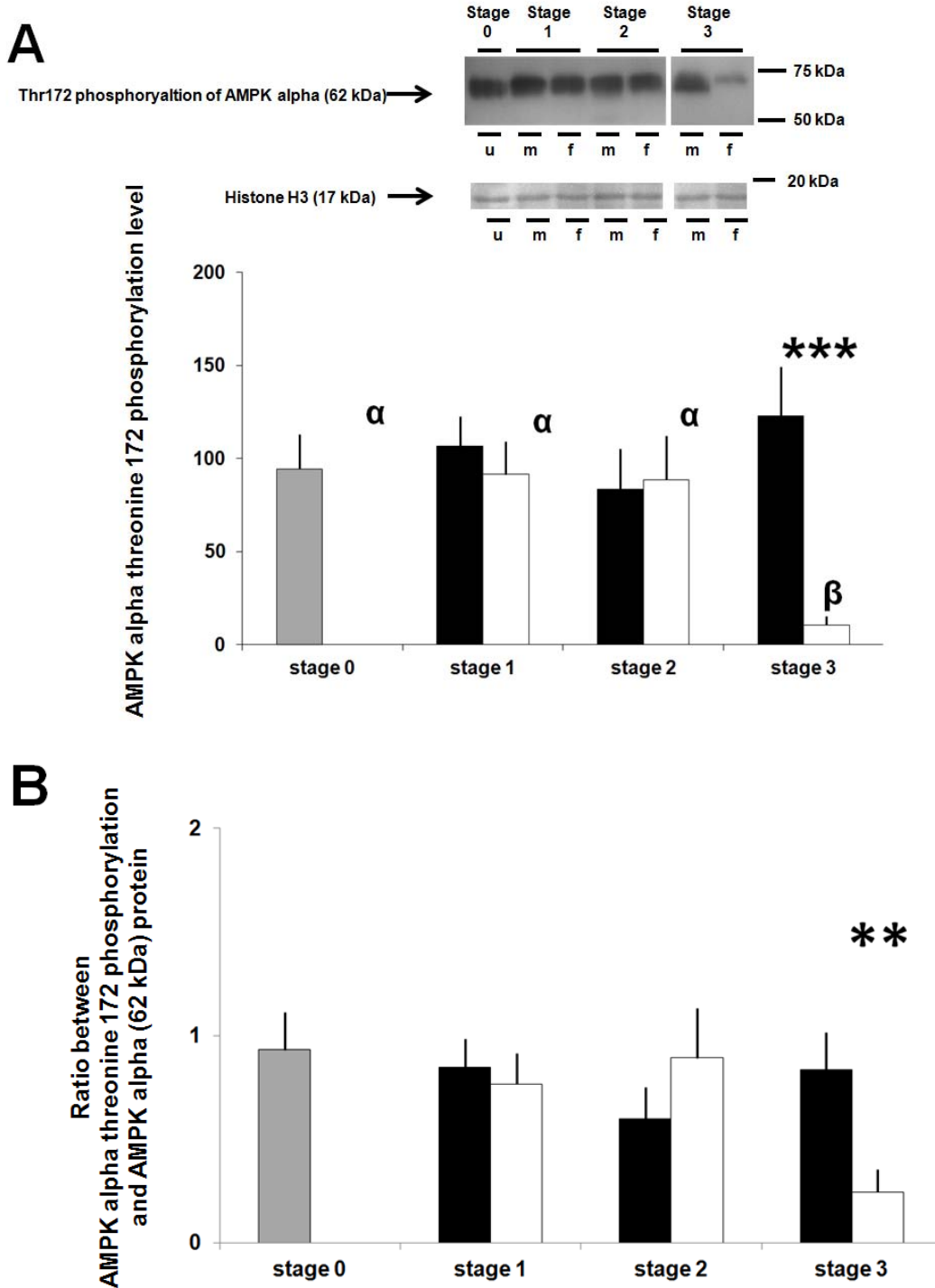
Figure 6: Relative levels of *ACC* (A), *NCOA4* (B), *CAMK4* (C) and *SREBP1* (D) transcripts in the gonad according to four different reproductive stages and sexes. Results are expressed as number of copies per copy of *efl*. Gray bar: sexually undifferentiated oysters (n = 13). Black bars: males (n = 10). White bars: females (n = 10). Columns and bars show mean ± SE. Different letters indicate a significant difference between stages. Asterisks indicate a significant difference between males and females, with $p < 0.05$ (*) or $p < 0.01$ (**).
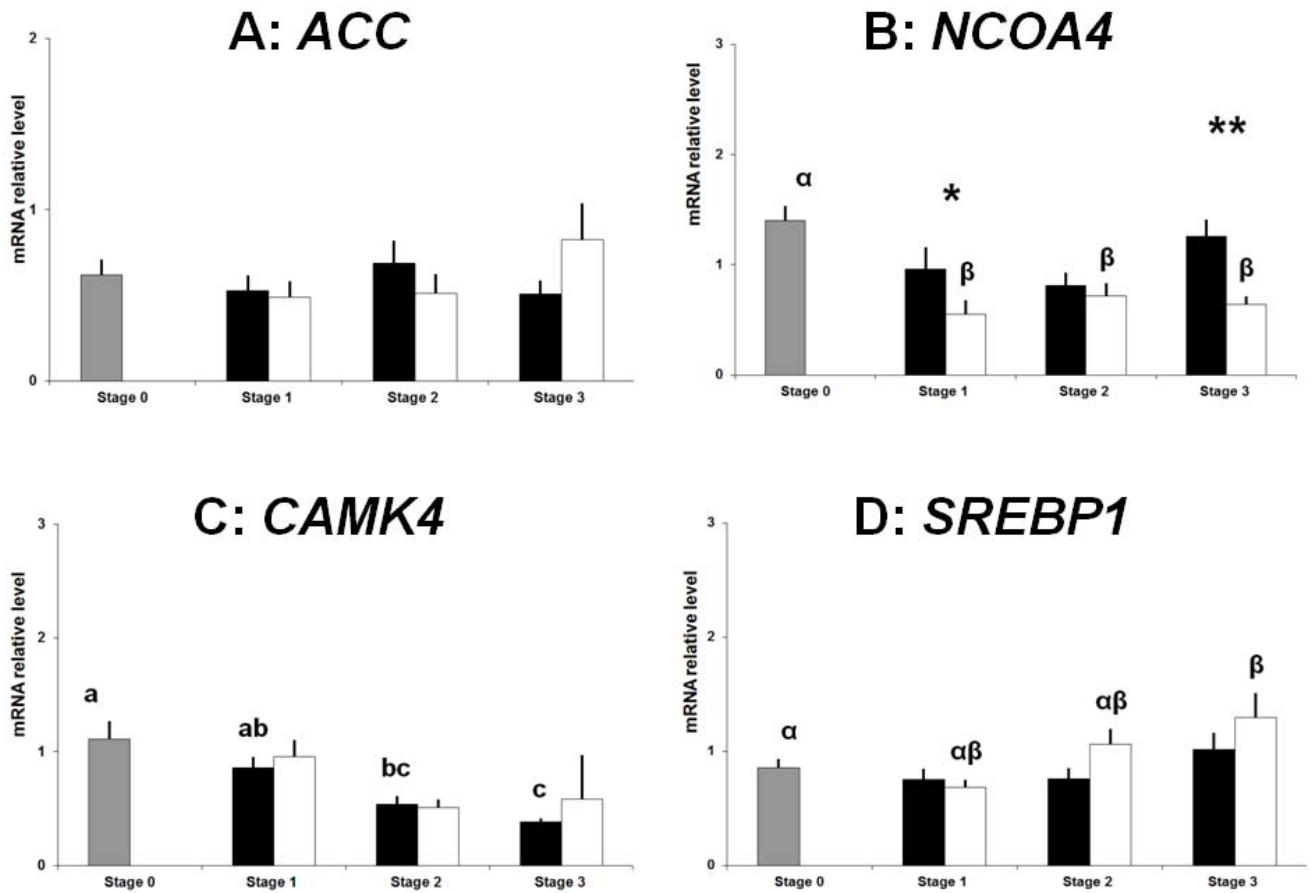
Figure 7: Relative levels of *PI3K* (A), *AKT* (B), and *CREB* (C) transcripts in the gonad according to sex and four different reproductive stages. Results are expressed as number of copies per copy of efI. Gray bar: sexually undifferentiated oysters (n = 13). Black bars: males (n = 10). White bars: females (n = 10). Columns and bars show mean ± SE. Different letters indicate a significant difference between stages. Asterisks indicate a significant difference between males and females, with $p < 0.05$ (*) or $p < 0.001$ (***).